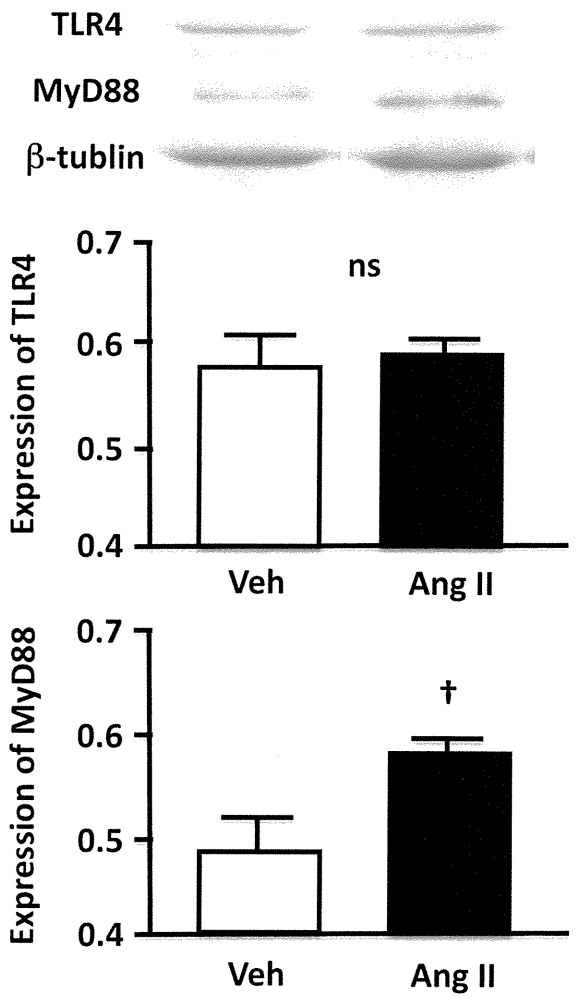

FIGURE 5. Twenty-four–hour urinary norepinephrine excretion as an indicator of activity of the SNS in the Ang II and Veh groups (†$P < 0.05$ vs. Veh group, n = 4 for each group). Data are shown as mean ± standard error of the mean.

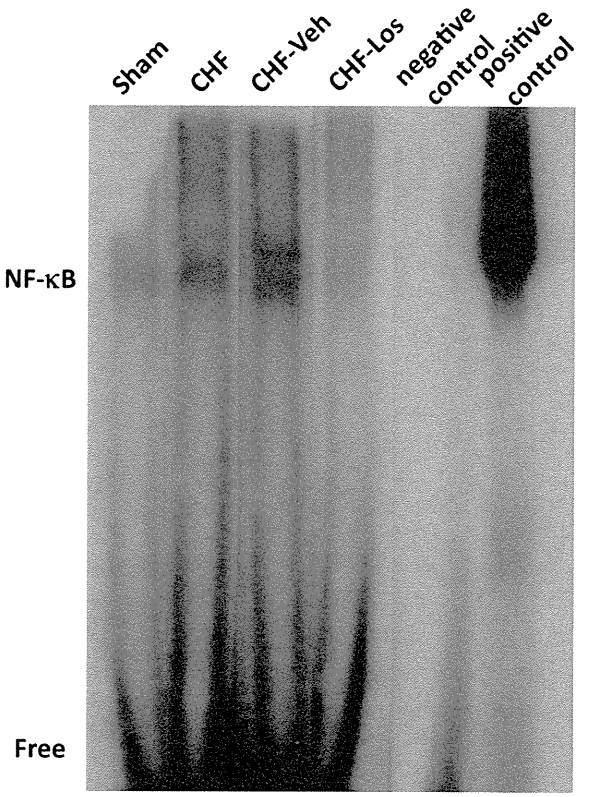

FIGURE 6. Western blots demonstrating the expression levels of the TLR and MyD88 in the brainstem in the Ang II group and Veh group (†$P < 0.05$ vs. Veh group, n = 4, for each group). Data are expressed as the ratio to the expression of the β-tubulin. Data are shown as mean ± standard error of the mean.

inflammation mediated by the TLR4 and MyD88 in the brainstem is in part involved in the sympathetic hyperactivity and LV remodeling in the MI-induced HF and might be a new target of the treatment of the MI-induced HF (Fig. 7).

Accumulating evidence indicates that the RAS in the brain contributes to the activation of the SNS via reactive oxygen species (ROS).[7,9,11,12,18,29,30,35] Previous studies have suggested that the RAS activates the SNS via brain ROS in the MI-induced HF.[7,9,11,12] Interestingly, we have demonstrated that inducible NOS, a key enzyme of the inflammation, in the brain activates the SNS[13,16] and that the AT_1R in the brain activates the SNS through the neural apoptosis in hypertensive model rats.[18] Based on these findings, we consider that the inflammatory cascade via ROS induced by the AT_1R in the brain might activate the SNS. In fact, we found that the enhanced expression level of the NF-κB was decreased after the blockade of the AT_1R in the brain of the MI-induced HF mice. Although we did not measure the oxidative stress in the brainstem of the MI-induced HF mice and did not determine the relationship between ROS and TLR4 in the present study, previous studies have indicated that the AT_1R in the brainstem activates the SNS via ROS in the MI-induced HF.[7,9,11,12] Therefore, it is possible that the inflammation mediated by the TLR4 and MyD88 in the brain might be one of the key mediators in the sympathoexcitation via ROS in the brain of the MI-induced HF mice.

The important finding of the present study was that central inhibition of the AT_1R in the brain reduced the expression levels of the TRL4 and MyD88 and the activity of the SNS, thereby improving the remodeling process in the MI-induced HF. A previous report suggests that the pharmacological systemic inhibition of the MyD88 protected against the LV dilatation and hypertrophy, and this protection occurred despite no measurable reduction in infarct size.[36] In the present study, we infused the AT_1R blocker or angiotensin II into the brain by the ICV infusion and did not determine the exact site in which these agents affect the brain. The dose of losartan and angiotensin II used in the present study was insufficient to act peripherally. There are several important autonomic nuclei in the central nervous system, including the brainstem nuclei and the hypothalamus,[37,38] and the AT_1R in the brain distributes richly in those nuclei.[39–41] Furthermore, the AT_1Rs in those nuclei are upregulated, associated with the sympathoexcitation in the MI-induced HF.[7,9,11,12] Therefore, it is possible

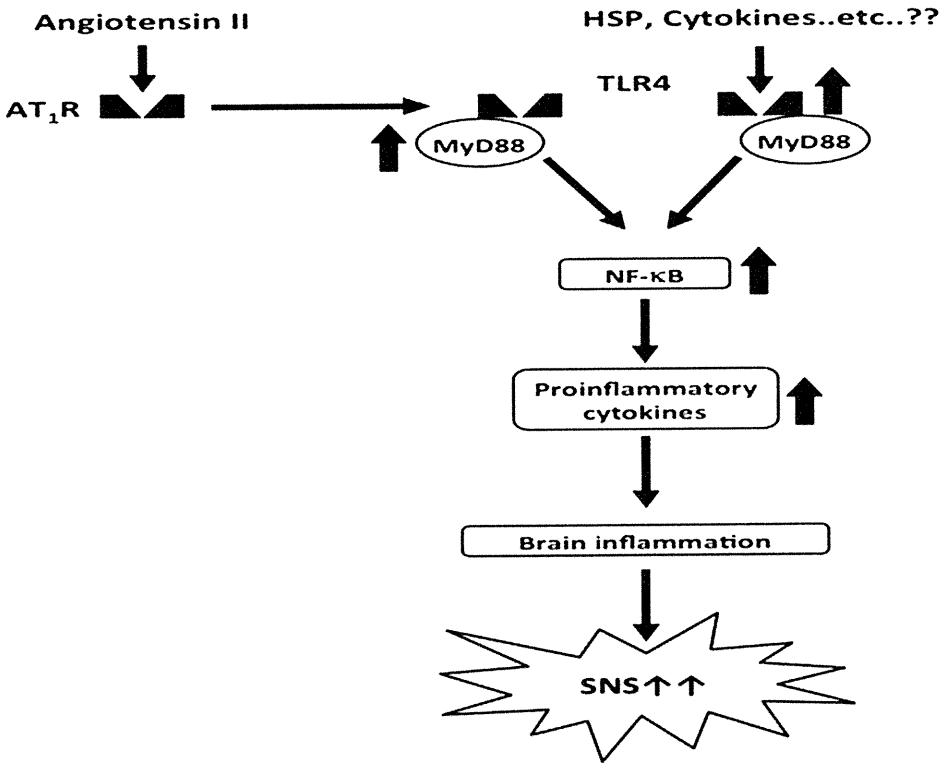

FIGURE 7. The scheme showing the cascade suggested by the results of the present study.

that activation of the AT_1R in those nuclei deteriorates the cardiac remodeling process through the TLR4 and MyD88 signaling. We suppressed the AT_1R–TLR4 pathway by the ICV infusion of the AT_1R blocker only for 14 days, and the activity of the SNS might be inhibited only for several days. We consider that the improvement of the LV function might need for longer period, at least for several months.

A previous report suggested that the ICV infusion of lipopolysaccharide (LPS), an agonist of the TLR4, elicits the activation of the SNS via proinflammatory cytokines and that the LPS increases the expression level of the AT_1R, NAD(P)H oxidase activity, and MAPK activity.[17] Other studies indicate that the blockade of the AT_1R decreases the expression level of the TLR4 in mesangial and smooth muscle cells.[31–34] In addition, we previously demonstrated that the AT_1R–NAD(P)H oxidase–MAPK pathway in the brainstem activates the SNS.[18] In the present study, we demonstrated that the ICV infusion of the AT_1R blocker inhibits the expression levels of the TLR4, MyD88, and NF-κB with sympathoinhibition and that the ICV infusion of the exogenous angiotensin II increases the expression level of the MyD88 with sympathoexcitation. Together with these previous and our findings, we consider that the upstream of the inflammation mediated by the TLR4 and MyD88 in the brain might be the AT_1R.

STUDY LIMITATIONS

There are some limitations in the present study. First, we did not show the direct evidence that the suppression of the AT_1R or TLR4 only in the brain reduced the enhanced central sympathetic outflow in the MI-induced HF because no agents for pharmacological inhibition of the TLR4 are available. Actually, there are already several studies of the MI-induced HF in the systemic *TLR4* gene knockout mice.[42,43] To gain a better understanding of the AT_1R-mediated TLR4 activation related to sympathoexcitation in MI-induced HF, future experiments using the genetically *TLR4* knockout mice will be needed. Second, we did not determine the ligand of the TLR4 in the present study. It has been suggested that not only LPS but also heat-shock protein or matrix components, such as fibronectin, hyaluronic acid, and fragments of heparan sulfate, have been reported to activate the TLR4[44] and that heat-shock protein 60 was in plasma after the ligation of LCA.[45] Further studies are necessary to examine the endogenous ligands of the TLR4 in the brain of the MI-induced HF mice.

CONCLUSIONS

In conclusion, our findings suggest that activation of the AT_1R in the brainstem enhances the central sympathetic outflow through at least in part the inflammation mediated by the TLR4 and MyD88 in mice with MI-induced HF (Fig. 7).

ACKNOWLEDGMENTS

This study was supported by a Grant-in-Aid for Scientific Research from the Japan Society for the Promotion of Science (B193290231, 33790709, and S23220013), and, in part, a Kimura Memorial Foundation Research Grant.

REFERENCES

1. Meredith IT, Eisenhofer G, Lambert GW, et al. Cardiac sympathetic nervous activity in congestive heart failure. Evidence for increased neuronal norepinephrine release and preserved neuronal uptake. *Circulation*. 1993;88:136–145.
2. Francis GS. The relationship of the sympathetic nervous system and the renin-angiotensin system in congestive heart failure. *Am Heart J*. 1989; 118:642–648.
3. Packer M. The neurohormonal hypothesis: a theory to explain the mechanism of disease progression in heart failure. *J Am Coll Cardiol*. 1992; 20:248–254.
4. Eichhorn EJ, Bristow MR. Medical therapy can improve the biological properties of the chronically failing heart. A new era in the treatment of heart failure. *Circulation*. 1996;94:2285–2296.
5. Goldsmith SR. Angiotensin II and sympathoactivation in heart failure. *J Cardiac Fail*. 1999;5:139–145.
6. Liu JL, Zucker IH. Regulation of sympathetic nerve activity in heart failure: a role for nitric oxide and angiotensin II. *Circ Res*. 1999;84:417–423.
7. Gao L, Wang W, Li YL, et al. Superoxide mediates sympathoexcitation in heart failure: roles of angiotensin II and NAD(P)H oxidase. *Circ Res*. 2004;95:937–944.
8. Murakami H, Liu JL, Zucker IH. Angiotensin II blockade [corrected] enhances baroreflex control of sympathetic outflow in heart failure. *Hypertension*. 1997;29:564–569.
9. Lindley TE, Doobay MF, Sharma RV, et al. Superoxide is involved in the central nervous system activation and sympathoexcitation of myocardial infarction-induced heart failure. *Circ Res*. 2004;94:402–409.
10. Liu D, Gao L, Roy SK, et al. Neuronal angiotensin II type 1 receptor upregulation in heart failure: activation of activator protein 1 and Jun N-terminal kinase. *Circ Res*. 2006;99:1004–1011.
11. Ahmad M, White R, Tan J, et al. Angiotensin-converting enzyme inhibitors, inhibition of brain and peripheral angiotensin-converting enzymes, and left ventricular dysfunction in rats after myocardial infarction. *J Cardiovasc Pharmacol*. 2008;51:565–572.
12. Zucker IH, Schultz HD, Patel KP, et al. Regulation of central angiotensin type 1 receptors and sympathetic outflow in heart failure. *Am J Physiol Heart Circ Physiol*. 2009;297:H1557–H1566.
13. Kimura Y, Hirooka Y, Kishi T, et al. Role of inducible nitric oxide synthase in rostral ventrolateral medulla in blood pressure regulation in spontaneously hypertensive rats. *Clin Exp Hypertens*. 2009;31:281–286.
14. Yu Y, Zhang ZH, Wei SG, et al. Brain perivascular macrophages and the sympathetic response to inflammation in rats after myocardial infarction. *Hypertension*. 2010;55:652–659.
15. Marvar PJ, Thabet SR, Guzik TJ, et al. Central and peripheral mechanisms of T-lymphocyte activation and vascular inflammation produced by angiotensin II-induced hypertension. *Circ Res*. 2010;107:263–270.
16. Kimura Y, Hirooka Y, Sagara Y, et al. Overexpression of inducible nitric oxide synthase in rostral ventrolateral medulla causes hypertension and sympathoexcitation via an increase in oxidative stress. *Circ Res*. 2005;96: 252–260.
17. Zhang ZH, Yu Y, Wei SG, et al. Centrally administered lipopolysaccharide elicits sympathetic excitation via NAD(P)H oxidase-dependent mitogen-activated protein kinase signaling. *J Hypertens*. 2010;28:806–816.
18. Kishi T, Hirooka Y, Konno S, et al. Angiotensin II type 1 receptor-activated caspase-3 through ras/mitogen-activated protein kinase/ extracellular signal-regulated kinase in the rostral ventrolateral medulla is involved in sympathoexcitation in stroke-prone spontaneously hypertensive rats. *Hypertension*. 2010;55:291–297.
19. Akira S, Takeda K. Toll-like receptor signalling. *Nat Rev*. 2004;4: 499–511.
20. Caso JR, Pradillo JM, Hurtado O, et al. Toll-like receptor 4 is involved in brain damage and inflammation after experimental stroke. *Circulation*. 2007;115:1599–1608.
21. Alfonso-Loeches S, Pascual-Lucas M, Blanco AM, et al. Pivotal role of TLR4 receptors in alcohol-induced neuroinflammation and brain damage. *J Neurosci*. 2010;30:8285–8295.
22. Gorina R, Font-Nieves M, Marquez-Kisinousky L, et al. Astrocyte TLR4 activation induces a proinflammatory environment through the interplay between MyD88-dependent NFkB signaling, MAPK, and Jak1/Stat1 pathways. *Glia*. 2011;59:242–255.
23. Lehnardt S, Massillon L, Follett P, et al. Activation of innate immunity in the CNS triggers neurodegeneration through a toll-like receptor 4-dependent pathway. *Proc Natl Acad Sci U S A*. 2003;100:8514–8519.
24. Wolf G, Bohlender J, Bondeva T, et al. Angiotensin II upregulates toll-like receptor 4 on mesangial cells. *J Am Soc Nephrol*. 2006;17: 1585–1593.
25. Wu J, Yang X, Zhang YF, et al. Angiotensin II upregulates toll-like receptor 4 and enhances lipopolysaccharide-induced CD40 expression in rat peritoneal mesothelial cells. *Inflamm Res*. 2009;58:473–482.
26. Lazartigues E, Sinnayah P, Augoyard G, et al. Enhanced water and salt intake in transgenic mice with brain-restricted overexpression of angiotensin (AT1) receptors. *Am J Physiol*. 2008;295:R1539–R1545.
27. Kishi T, Hirooka Y, Sakai K, et al. Overexpression of eNOS in the RVLM causes hypotension and bradycardia via GABA release. *Hypertension*. 2001;38:896–901.
28. Kishi T, Hirooka Y, Ito K, et al. Cardiovascular effects of overexpression of endothelial nitric oxide synthase in the rostral ventrolateral medulla in stroke-prone spontaneously hypertensive rats. *Hypertension*. 2002;39: 264–268.
29. Kishi T, Hirooka Y, Kimura Y, et al. Increased reactive oxygen species in rostral ventrolateral medulla contribute to neural mechanisms of hypertension in stroke-prone spontaneously hypertensive rats. *Circulation*. 2004;109:3257–3262.
30. Zimmerman MC, Lazartigues E, Sharma RV, et al. Hypertension caused by angiotensin II infusion involves increased superoxide production in the central nervous system. *Circ Res*. 2004;95:210–216.
31. Yang J, Jiang H, Yang J, et al. Valsartan preconditioning protects against myocardial ischemia-reperfusion injury through TLR4/NF-kB signaling pathway. *Mol Cell Biochem*. 2009;330:39–46.
32. Dasu MR, Riosvelasco AC, Jialal I. Candesartan inhibits toll-like receptor expression and activity both in vitro and in vivo. *Atherosclerosis*. 2009;202:76–83.
33. Lv J, Jia R, Yang D, et al. Candesartan attenuates angiotensin II-induced mesangial cell apoptosis via TLR4/MyD88 pathway. *Biochem Biophys Res Commun*. 2009;380:81–86.
34. Cheng XW, Song H, Sasaki T, et al. Angiotensin type 1 receptor blocker reduces intimal neovascularization and plaque growth in apolipoprotein E-deficient mice. *Hypertension*. 2011;57:981–989.
35. Hirooka Y, Kishi T, Sakai K, et al. Imbalance of central nitric oxide and reactive oxygen species in the regulation of sympathetic activity and neural mechanisms of hypertension. *Am J Physiol*. 2011;300: R818–R826.
36. Van Tassell BW, Seropian IM, Toldo S, et al. Pharmacologic inhibition of myeloid differentiation factor 88 (MyD88) prevents left ventricular dilation and hypertrophy after experimental acute myocardial infarction in the mouse. *J Cardiovasc Pharmacol*. 2010;55:385–390.
37. Dampney RAL. Functional organization of central pathways regulating the cardiovascular system. *Physiol Rev*. 1994;74:323–364.
38. Guyenet PG. The sympathetic control of blood pressure. *Nat Rev Neurosci*. 2006;7:335–346.
39. McKinley MJ, Albinson AL, Allen AM, et al. The brain renin-angiotensin system: location and physiological roles. *Int J Biochem Cell Biol*. 2003;35: 901–918.
40. Dupont AG, Brouwers S. Brain angiotensin peptides regulate sympathetic tone and blood pressure. *J Hypertens*. 2010;28:1599–1610.
41. Allen AM, O'Callaghan EL, Chen D, et al. Central neural regulation of cardiovascular function by angiotensin: a focus on the rostral ventrolateral medulla. *Neuroendocrinology*. 2009;89:361–369.
42. Wang E, Feng Y, Zhang M, et al. Toll-like receptor 4 signaling confers cardiac protection against ischemic injury via inducible nitric oxide synthase- and soluble guanylate cyclase-dependent mechanisms. *Anesthesiology*. 2011;114:603–613.
43. Riad A, Jäger S, Sobirey M, et al. Toll-like receptor-4 modulates survival by induction of left ventricular remodeling after myocardial infarction in mice. *J Immunol*. 2008;180:6954–6961.
44. Takeda K, Kaisho T, Akira S. Toll-like receptors. *Annu Rev Immunol*. 2003;21:335–376.
45. Lin L, Kim SC, Wang Y, et al. HSP60 in heart failure: abnormal distribution and role in cardiac myocyte apoptosis. *Am J Physiol*. 2007;293: H2238–H2247.

Neuregulin-1/ErbB signaling in rostral ventrolateral medulla is involved in blood pressure regulation as an antihypertensive system

Ryuichi Matsukawa[a], Yoshitaka Hirooka[b], Masaaki Nishihara[a], Koji Ito[a] and Kenji Sunagawa[a]

Objectives Neuregulin-1 (NRG-1), located in the central nervous system (CNS), plays an important role in synaptic function, neurite outgrowth, and survival of neurons and glia acting on the ErbB receptor family. However, the functional role of NRG-1/ErbB signaling in the CNS and blood pressure regulation is unknown, particularly in the rostral ventrolateral medulla (RVLM), a major vasomotor center. Thus, we investigated whether NRG-1/ErbB signaling in the RVLM is involved in blood pressure regulation.

Methods and results Microinjection of NRG-1 into the RVLM decreased arterial blood pressure, heart rate (HR), and renal sympathetic nerve activity (RSNA) in Wistar rats. In contrast, microinjection of an ErbB2 or ErbB4 inhibitor into the RVLM increased arterial pressure, HR, and RSNA. ErbB2 expression levels in the brainstem were significantly lower in spontaneously hypertensive rats (SHRs) than in Wistar–Kyoto (WKY) rats. Depressor responses to NRG-1 and pressor responses to the ErbB2 inhibitor were significantly smaller in SHRs than in WKY rats ($P<0.05$). Furthermore, the inhibition of ErbB2 expression in the RVLM by RNA interference significantly increased arterial pressure, HR, and urinary norepinephrine excretion in conscious WKY rats ($P<0.01$).

Conclusion Our findings indicate that the NRG-1/ErbB signaling in the RVLM has depressor and sympathoinhibitory effects. Reduced NRG/ErbB2 signaling in the RVLM may contribute to the neural mechanisms of hypertension. *J Hypertens* 29:1735–1742 © 2011 Wolters Kluwer Health | Lippincott Williams & Wilkins.

Journal of Hypertension 2011, 29:1735–1742

Keywords: blood pressure, ErbB, hypertension, neuregulin-1, rostral ventrolateral medulla, sympathetic nervous system

Abbreviations: CNS, central nervous system; GABA, γ-aminobutyric acid; HR, heart rate; MAP, mean arterial pressure; NRG-1, neuregulin-1; RSNA, renal sympathetic nerve activity; RVLM, rostral ventrolateral medulla; SHR, spontaneous hypertensive rat; siRNA, small-interference RNA; uNE, urinary norepinephrine excretion; WKY, Wistar–Kyoto

[a]Department of Cardiovascular Medicine and [b]Department of Advanced Cardiovascular Regulation and Therapeutics, Kyushu University Graduate School of Medical Sciences, Fukuoka, Japan

Correspondence to Yoshitaka Hirooka, MD, PhD, FAHA, Department of Advanced Cardiovascular Regulation and Therapeutics, Kyushu University Graduate School of Medical Sciences, 3–1–1 Maidashi, Higashi-ku, Fukuoka 812–8582, Japan
Tel: +81 92 6425356; fax: +81 92 6425374;
e-mail: hyoshi@cardiol.med.kyushu-u.ac.jp

Received 23 March 2011 **Revised** 23 May 2011
Accepted 25 May 2011

Introduction

Neuregulin-1 (NRG-1) is a member of the epidermal growth factor family, which is involved in cell–cell communication [1,2]. NRG-1 is expressed in the nervous system, heart, and other organ systems [1–3]. NRG-1 binds to the extracellular domain of the tyrosine kinase ErbB3 or ErbB4, which often leads to the formation of ErbB heterodimers with ErbB2. This activates intracellular signaling pathways leading to synaptic function, neurite outgrowth, and survival of neurons and glia [3–5]. It is also known that NRG-1 and ErbB receptors are widely distributed in the central nervous system (CNS), including the brainstem [6–10]. Several studies have demonstrated the involvement of NRG-1/ErbB signaling in the regulation of neurotransmitters, such as L-glutamate and γ-aminobutyric acid (GABA) [11,12]. In addition, ErbB2 is known to be involved in the development of glial cells and their transformation into astrocytes [13]. However, little is known regarding the role of the NRG-1/ErbB signaling pathway in the brainstem and the action of this pathway on blood pressure regulation.

With regard to CNS blood pressure regulation, the rostral ventrolateral medulla (RVLM) of the brainstem is one of the most important regions involved in central cardiovascular regulation [14–17]. RVLM neurons project toward sympathetic preganglionic neurons in the intermediolateral cell column of the spinal cord and provide an essential excitatory drive, thereby maintaining sympathetic vasomotor tone [14]. In addition, the RVLM neurons regulate sympathetic vasomotor tone by integrating the inputs from baroreceptors, chemoreceptors, and higher autonomic nuclei [18]. Accumulating evidence suggests that increased RVLM activity leads to chronic sympathetic hyperactivity in many forms of hypertension [17]. For example, in spontaneously hypertensive rats (SHRs), excitation of the RVLM vasomotor

0263-6352 © 2011 Wolters Kluwer Health | Lippincott Williams & Wilkins DOI:10.1097/HJH.0b013e32834937d6

neurons is increased by L-glutamate-mediated excitation and decreased GABA-mediated inhibition [16,17]. Therefore, the aim of the present study was to determine whether NRG-1/ErbB signaling in the RVLM contributes to blood pressure regulation through the sympathetic nervous system, and, if so, whether alteration of this signaling in the RVLM occurs in SHRs, leading to the activation of the sympathetic nervous system associated with neurogenic hypertensive mechanisms. We investigated the effect of NRG-1 and the ErbB receptor blockers injected into the RVLM on arterial blood pressure, heart rate (HR), and sympathetic nervous system activity. Expression levels of NRG-1 and ErbB receptors were also evaluated. These effects were examined in SHRs to elucidate the role of this signaling in hypertension. Finally, we further examined the effects of this signaling in conscious rats using small-interference RNA (siRNA) techniques.

Methods

This study was reviewed and approved by the Committee on Ethics of Animal Experiments, Kyushu University Graduate School of Medical Sciences, and it was performed according to the Guidelines for Animal Experiments of Kyushu University.

Microinjection studies

Animals were anesthetized and measured for arterial pressure, HR and renal sympathetic nerve activity (RSNA). For details of general surgical preparation, see online Data Supplemental Digital Content 1, http://links.lww.com/HJH/A108. Microinjections into the RVLM were made according to the following protocols: unilateral microinjection of recombinant NRG-1β (NRG-1β: 0.025, 0.25, and 2.5 pmol in 50 nl injections; Ray Biotech, Norcross, Georgia, USA) in Wistar rats and NRG-1β (2.5 pmol in 50 nl injections) was microinjected in Wistar–Kyoto (WKY) rats and SHRs; bilateral microinjections of the ErbB2 antagonists AG825 (0.5 pmol in 50 nl injections; Santa Cruz Biotechnology, Santa Cruz, California, USA) in Wistar rats, WKY rats, and SHRs; bilateral microinjections of the ErbB4 antagonists AG1478 (0.5 pmol in 50 nl injections; Santa Cruz Biotechnology) in Wistar rats, WKY rats, and SHRs; unilateral microinjection of NRG-1β (2.5 pmol in 50 nl injections) 10 min after unilateral injection of both AG825 (0.5 pmol in 50 nl injections) and AG1478 (0.5 pmol in 50 nl injections) in Wistar rats; unilateral microinjection of NRG-1β (2.5 pmol in 50 nl injections) 5 min after unilateral injection of the GABA-A receptor antagonist bicuculline (100 pmol in 50 nl injections; Santa Cruz) in Wistar rats; and unilateral microinjection of L-glutamate (1.0 nmol in 50 nl injections; Nakarai Tesque, Fukuoka, Japan) 10 min after unilateral injection of NRG-1β (2.5 pmol in 50 nl injections) in Wistar rats. Arterial pressure, HR, and RSNA are monitored in the first (2.5 pmol NRG-1β), second, and third protocol. Arterial pressure and HR are monitored in the first (0.025 and 0.25 pmol NRG-1β) and the fourth to sixth protocol. Dosages of reagents were determined as follows. The dose of NRG-1β was determined on the basis of previous studies [19,20]. Additionally, we confirmed the dose response in the present study. Doses of AG825 and AG1478 were determined on the basis of previous studies and half maximal inhibitory concentration (IC_{50}) values [21–25]. Furthermore, to exclude the peripheral effects of the agents, we performed intravenous administration of the agents (the same amount of the agents used in microinjection studies in 0.2 ml isotonic saline). However, there were no effects on mean arterial pressure (MAP) and HR [ΔMAP: NRG-1 (2.5 pmol), -0.9 ± 1.8 mmHg; AG825 (1.0 pmol), 0.6 ± 1.8 mmHg; AG1478 (1.0 pmol), 0.3 ± 1.1 mmHg; and ΔHR: NRG-1, 0.6 ± 2.3 beats/min; AG825, 0.9 ± 2.8 beats/min; AG1478, 1.0 ± 0.9 beats/min ($n = 3$ for each)]. Doses of bicuculline and L-glutamate were determined on the basis of previous studies [26–28].

Western blot analysis

Western blots were made according to the following protocols: first, expressions of NRG-1 and ErbB receptors (ErbB2, ErbB3, and ErbB4) in the brainstem of 4-week-old and 12-week-old WKY rats and SHRs were confirmed. Rabbit IgG monoclonal antibodies against NRG-1 (1 : 1000), ErbB2 (1 : 1000), ErbB3 (1 : 1000), and ErbB4 (1 : 1000) were used as the primary antibody. Additionally, expression of ErbB2 in the cerebral cortex or hypothalamus of 12-week-old WKY rats and SHRs was confirmed. Second, in a study of chronic inhibition of ErbB2 in the RVLM by siRNA, western blot was performed to confirm the effects of RNA interference on the ErbB2 receptor using RVLM tissues of WKY rats. At 0, 1, 5, and 14 days after administration of ErbB2 or control siRNA (siErbB2 or siControl), rats were anesthetized using sodium pentobarbital and perfused transcardially with PBS. RVLM tissues defined according to a rat brain atlas were obtained as previously described [29]. Anti-ErbB2 antibody (1 : 1000) was used. For details see online Data Supplemental Digital Content 1, http://links.lww.com/HJH/A108.

In-vivo small-interference RNA technique

The siErbB2 sequence was determined as described in a previous study [30]. Specific siErbB2 (AAGUGUGUG UACCGGCACAGACA) and scrambled siRNA (siControl: AGCCUAACUGAACGCGUAGGA), as a control, were purchased from Koken, Tokyo, Japan. Furthermore, we used the in-vivo siRNA delivery kit AteloGene (Koken) for stable local delivery of the siRNA into the RVLM. SiErbB2 or siControl was administered into the RVLM, and MAP and HR were monitored using radiotelemetry system for 14 days. For details see online Data Supplemental Digital Content 1, http://links.lww.com/HJH/A108.

Measurement of urinary norepinephrine excretion

We measured urinary norepinephrine excretion (uNE) concentration before and at 1, 7, and 14 days after the start of the administration of siRNA and calculated uNE as described previously [26,31].

Statistical analysis

All values are expressed as the mean ± SEM. Differences were considered significant when the P value was less than 0.05. For details see online Data Supplemental Digital Content 1, http://links.lww.com/HJH/A108.

Results

Baseline mean arterial pressure and heart rate of microinjection study

The baseline MAP and HR in microinjection protocols of NRG-1β, AG825, and AG1478 are described in Supplemental Digital Content 2, Online Table 1, http://links.lww.com/HJH/A109.

Effects of neuregulin-1 injection into the rostral ventrolateral medulla on arterial blood pressure, heart rate, and renal sympathetic nerve activity

Microinjection of NRG-1β (2.5 pmol) into the RVLM unilaterally significantly decreased MAP, HR, and RSNA [ΔMAP, −22.3 ± 1.8 mmHg; ΔHR, −36.1 ± 5.5 beats/min; ΔRSNA %baseline, −36.9 ± 6.2%; $P < 0.01$, $n = 5$; Fig. 1a]. These changes occurred slowly and peaked approximately 10–15 min after injection. The depressor and bradycardic responses induced by NRG-1β occurred in a dose-dependent manner (Fig. 1b).

Fig. 1

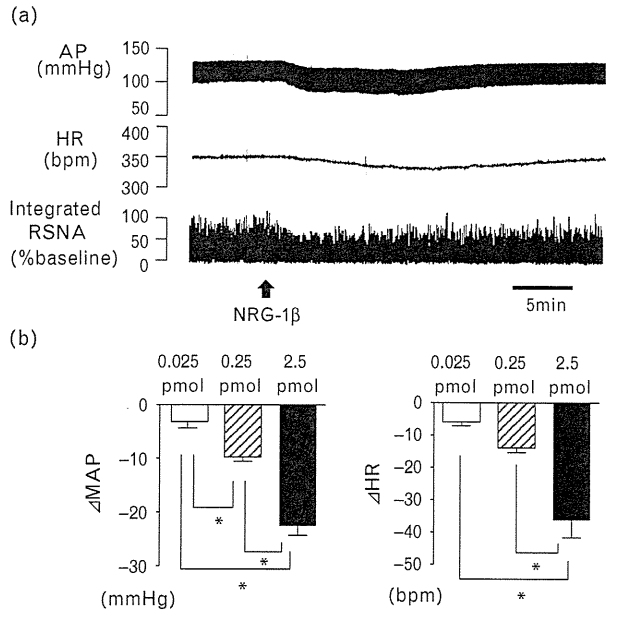

Response of arterial pressure (AP), heart rate (HR), and renal sympathetic nerve activity (RSNA) to unilateral microinjection of neuregulin-1β (NRG-1β) into the rostral ventrolateral medulla of Wistar rats. (a) Raw data of changes in AP, HR, and RSNA in response to microinjection of NRG-1β (2.5 pmol). (b) Group data of changes in mean AP (MAP) and HR in response to microinjection of NRG-1β. Values are expressed as mean ± SEM. *$P < 0.05$ ($n = 5$ per injection).

Effects of inhibition of ErbB2 and ErbB4 receptors in the rostral ventrolateral medulla on mean arterial pressure, heart rate, and renal sympathetic nerve activity

MAP, HR, and RSNA values increased significantly after bilateral injection of the ErbB2 receptor blocker, AG825 (1.0 pmol), into the RVLM (ΔMAP, +17.6 ± 2.3 mmHg; ΔHR, +16.5 ± 1.1 beats/min; ΔRSNA %baseline, +29.6 ± 4.1%; $P < 0.01$, $n = 5$; Fig. 2a, c). These variables also increased after injection of the ErbB4 inhibitor, AG1478 (1.0 pmol) (ΔMAP, 11.0 ± 1.6 mmHg; ΔHR, 12.9 ± 1.9 beats/min; ΔRSNA %baseline, +18.3 ± 3.8%; $P < 0.01$, $n = 5$; Fig. 2b, c). These changes occurred slowly and peaked approximately 10–15 min after microinjection of the blockers. After microinjection of both AG825 (0.5 pmol) and AG1478 (0.5 pmol), the depressor response to NRG-1β (2.5 pmol) injected into the RVLM was nearly abolished (ΔMAP, −22.3 ± 1.8 vs. −2.0 ± 0.7 mmHg; ΔHR, −36.1 ± 5.5 vs. −2.5 ± 0.7 beats/min; $P < 0.01$, $n = 5$ for each; Fig. 2d).

Furthermore, to demonstrate that the effects of the reagents in the RVLM are site specific, microinjections of NRG-1β and AG825 were performed 1.0-mm dorsal apart from the RVLM in Wistar rats. The changes in MAP, HR, and RSNA were not significant (Supplemental Digital Content 2, Online Table 2, http://links.lww.com/HJH/A109).

Effect of blockade of γ-aminobutyric acid-A receptors in the rostral ventrolateral medulla on the depressor response to neuregulin-1

The baseline MAP before NRG-1β injection increased after the injection of the GABA-A receptor antagonist bicuculline (100 pmol) (MAP increased from 118.3 ± 3.8 to 146.3 ± 10.7 mmHg, whereas HR decreased from 337.8 ± 13.2 to 332.3 ± 17.6 beats/min). The depressor response to NRG-1β (2.5 pmol) into the RVLM was significantly attenuated after bicuculline injection (ΔMAP, −22.9 ± 2.9 vs. −4.6 ± 2.0 mmHg; ΔHR, −38.1 ± 5.5 vs. −11.9 ± 2.3 beats/min; $P < 0.01$, $n = 5$ for each).

Effect of neuregulin-1 in the rostral ventrolateral medulla on the pressor response to L-glutamate

The baseline MAP before L-glutamate injection decreased after NRG-1β injection (2.5 pmol) from 126.0 ± 5.2 to 109.9 ± 4.3 mmHg. The pressor response to L-glutamate (1.0 nmol) into the RVLM was significantly attenuated after NRG-1β injection (ΔMAP, 23.4 ± 1.0 vs. 10.8 ± 1.6 mmHg; $P < 0.01$, $n = 5$ for each).

ErbB receptors expression levels in the brainstem in Wistar–Kyoto and spontaneously hypertensive rats

NRG-1 and ErbB receptors (ErbB2, ErbB3, and ErbB4) are expressed in the brainstem in both the 12-week-old

Fig. 2

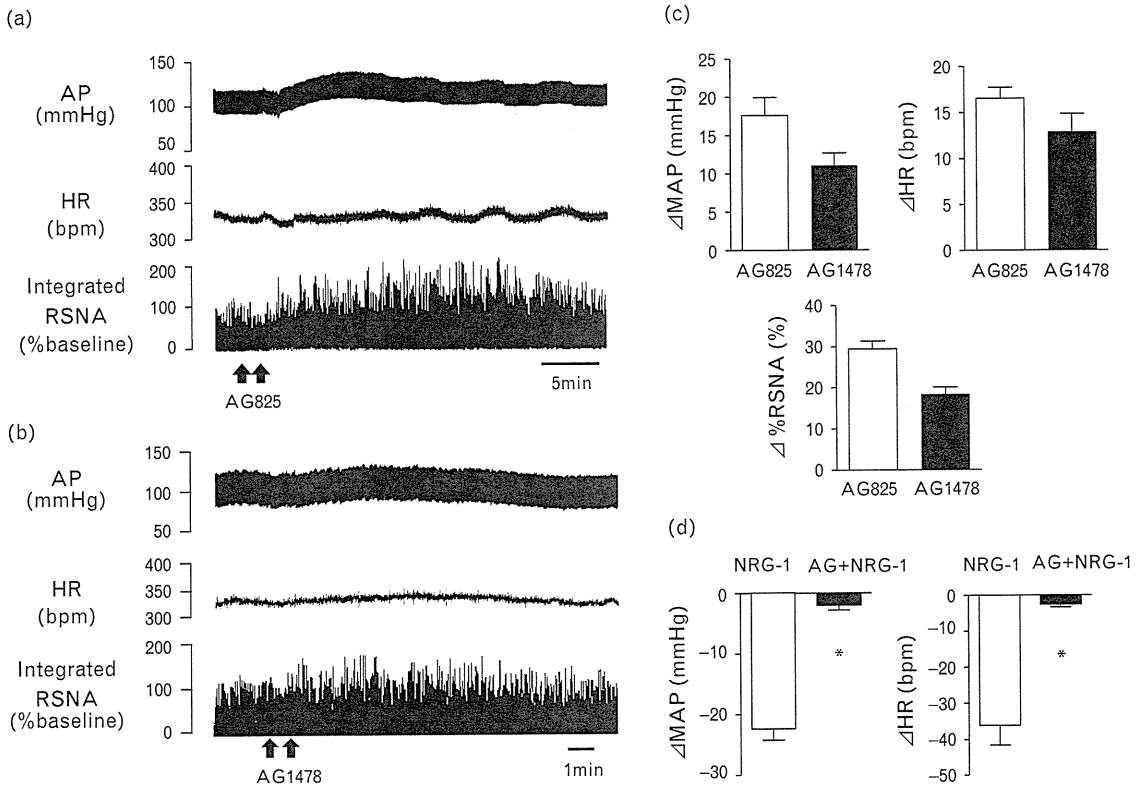

Response of arterial pressure (AP), heart rate (HR), and renal sympathetic nerve activity (RSNA) to bilateral microinjection of the ErbB2 antagonist (AG825) and ErbB4 antagonist (AG1478) into the rostral ventrolateral medulla (RVLM) of Wistar rats. (a) Raw data of changes in AP, HR, and RSNA response to microinjection of AG825 (1.0 pmol). (b) Raw data of changes in AP, HR, and RSNA response to microinjection of AG1478 (1.0 pmol). (c) Group data of changes in mean AP (MAP), HR, and RSNA in response to microinjection of AG825 or AG1478. Values are expressed mean ± SEM ($n = 5$ per injection). (d) Effect of blockade of both ErbB2 and ErbB4 receptors in the RVLM on the depressor response to NRG-1β. NRG-1 represents unilateral microinjection of neuregulin-1β (NRG-1β, 2.5 pmol) without pretreatment into the RVLM of Wistar rats and AG+NRG-1 represents unilateral microinjection of NRG-1β (2.5 pmol) with prior injection of both AG825 (0.5 pmol) and AG1478 (0.5 pmol) into the RVLM of Wistar rats. Values are expressed as mean ± SEM. $^*P < 0.05$ ($n = 5$ for each).

SHRs and WKY rats. However, only ErbB2 expression levels were significantly lower in SHRs than in WKY rats ($P < 0.05$, $n = 5$ for each; Fig. 3a). We further examined NRG-1 and ErbB receptor expression levels in the brainstem of 4-week-old prehypertensive SHRs and age-matched WKY rats. ErbB2 expression levels were significantly lower in 4-week-old SHRs than in WKY rats ($n = 5$ for each; Fig. 3a). NRG-1 and other ErbB receptor expression levels, however, were similar between SHRs and WKY rats for both ages ($n = 5$ for each; Fig. 3b). On the contrary, in cerebral cortex and hypothalamus, ErbB2 expression levels were similar between 12-week-old SHRs and WKY rats (Fig. 3c).

Acute effects of neuregulin-1 or ErbB inhibitors on mean arterial pressure in Wistar–Kyoto and spontaneously hypertensive rats

The magnitudes of decreases in MAP, HR, and RSNA evoked by the unilateral injection of NRG-1β (2.5 pmol) into the RVLM were significantly smaller in SHRs than in WKY rats (ΔMAP, -23.3 ± 2.5 vs. -12.5 ± 1.7 mmHg, $P < 0.01$; ΔHR, -29.9 ± 4.0 vs. -15.5 ± 1.6 beats/min, $P < 0.05$; ΔRSNA %baseline, -33.8 ± 4.2 vs. $-17.2 \pm 3.0\%$, $P < 0.01$; $n = 5$ for each; Fig. 4a). The magnitudes of increases in MAP, HR, and RSNA evoked by the injection of AG825 (1.0 pmol) were significantly smaller in SHRs than in WKY rats (ΔMAP, $+16.7 \pm 1.4$ vs. $+8.9 \pm 1.0$ mmHg, $P < 0.05$; ΔHR, $+20.5 \pm 4.2$ vs. $+10.0 \pm 1.2$ beats/min, $P < 0.05$; ΔRSNA %baseline, $+31.8 \pm 4.9$ vs. $+17.8 \pm 2.3\%$, $P < 0.01$; $n = 5$ for each; Fig. 4b). In contrast, the magnitudes of increase in MAP, HR, and RSNA evoked by the injection of AG1478 (1.0 pmol) did not differ between SHRs and WKY rats (ΔMAP, $+8.7 \pm 0.9$ vs. $+9.9 \pm 1.2$ mmHg; ΔHR, $+11.2 \pm 1.8$ vs. $+10.9 \pm 0.8$ beats/min; ΔRSNA %baseline, $+18.9 \pm 3.5$ vs. $+19.8 \pm 3.7\%$; $P =$ NS, $n = 5$; Fig. 4c).

Effects of local inhibition of ErbB2 in the rostral ventrolateral medulla caused by in-vivo small-interference RNA on mean arterial pressure, heart rate, and urinary norepinephrine excretion in conscious Wistar–Kyoto rats

Inhibition of ErbB2 receptors in the RVLM using siRNA increased MAP and HR between days 1 and 5

Fig. 3

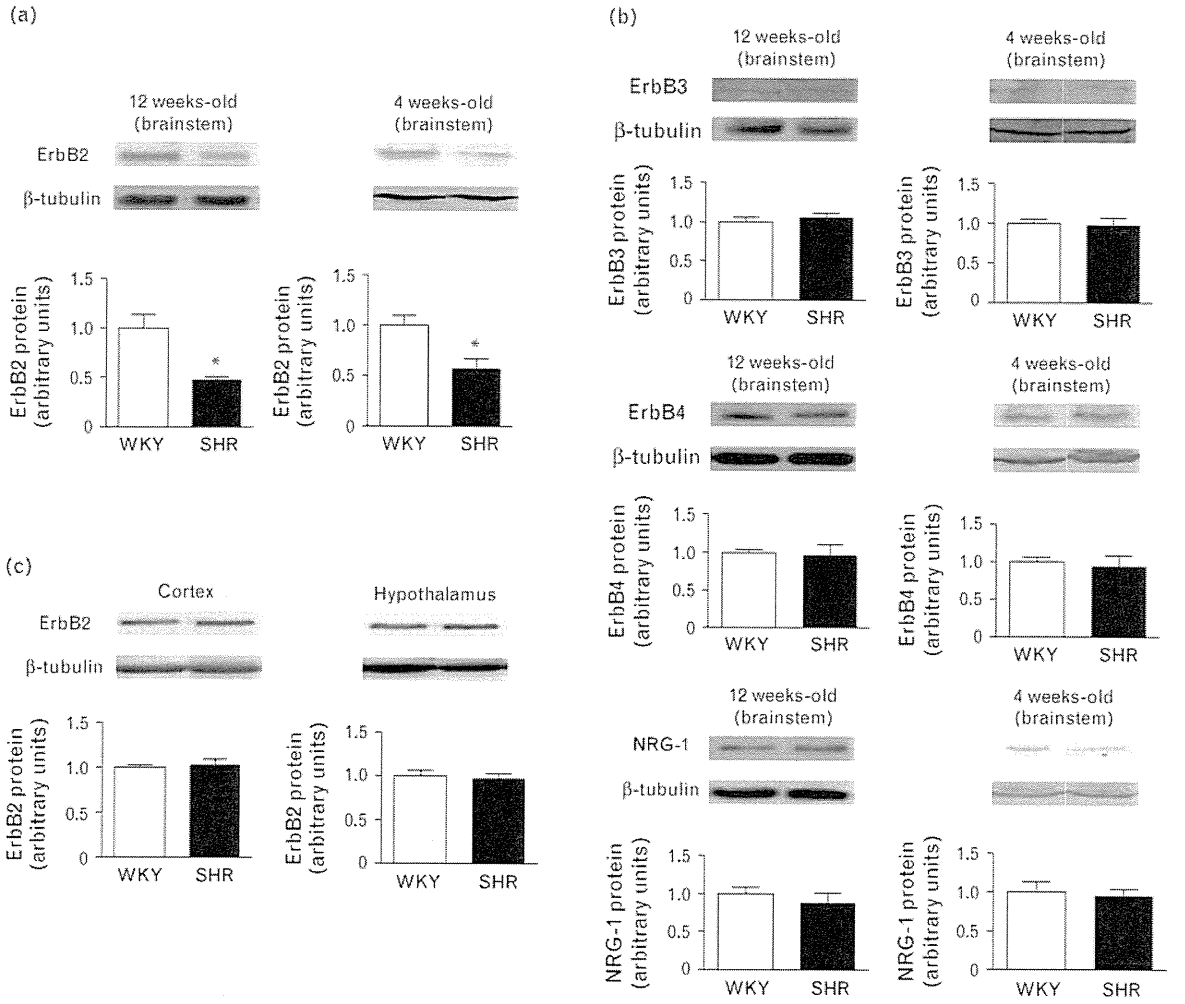

Western blot of (a) ErbB2, (b) neuregulin-1 (NRG-1), ErbB3, and ErbB4 in the brainstem of 12-week-old and 4-week-old Wistar–Kyoto (WKY) rats and spontaneously hypertensive rats (SHRs). (c) Western blot of ErbB2 in cerebral cortex and hypothalamus of 12-week-old WKY rats and SHRs. The densitometric average was normalized to the values obtained from the analysis of β-tubulin as internal control. Expressions are shown relative to that in WKY rats, which were assigned a value of 1. Values are expressed as mean ± SEM. $^*P < 0.05$ (vs. WKY rats, $n = 5$ for each).

after the siErbB2 treatment in WKY rats. In contrast, these variables did not change in the siControl-treated rats ($P < 0.05$, $n = 5$ for each; Fig. 5a). Twenty-four-hour uNE levels at day 1 and 7 were significantly greater in siErbB2 than that in siControl-treated rats ($P < 0.01$, $n = 5$ for each; Fig. 5b). The ErbB2 protein expression levels of RVLM in siErbB2-treated rats were successfully inhibited between days 1 and 5 compared with day 0 (Fig. 5c).

Discussion

The findings of the present study are the first to suggest that NGR-1/ErbB signaling in the RVLM reduces blood pressure through the inhibition of the sympathetic nervous system activity. This suggestion is supported by the results of microinjection of NRG-1 or ErbB2 and ErbB4 antagonists into the RVLM, which demonstrated a decrease or increase in blood pressure associated with changes in RSNA in acute anesthetized rats. This is further supported by the experiments involving the inhibition of ErbB2 receptors in the RVLM using siRNA for ErbB2 receptors in chronic conscious state. Furthermore, our findings suggest that signaling in the RVLM is impaired in SHRs. This is based on the results indicating that the depressor response to NRG-1 and pressor response to the ErbB2 in the RVLM are attenuated in SHRs together with the reduced ErbB2 expression levels in the RVLM of SHRs. Therefore, signaling abnormalities in the RVLM may contribute to, at least in part, the neurogenic mechanisms of hypertension.

NRG-1/ErbB signaling in the RVLM was found to have depressor effects with sympathoinhibition. Microinjection of recombinant NRG-1β into the RVLM decreased arterial pressure, HR, and RSNA in anesthetized normotensive rats. In contrast, microinjection of the ErbB2

Fig. 4

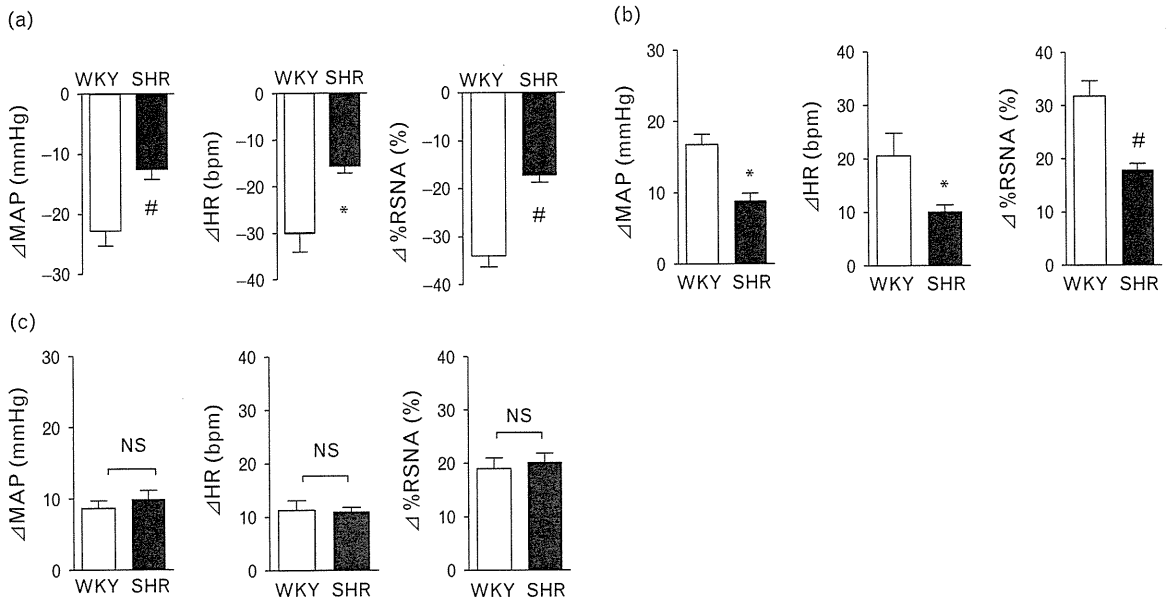

Comparison of responses of mean arterial pressure (MAP), heart rate (HR), and renal sympathetic nerve activity (RSNA) (%baseline) in 12-week-old Wistar–Kyoto (WKY) and spontaneously hypertensive rats to (a) unilateral injection of neuregulin-1β (2.5 pmol); (b) bilateral injection of AG825 (1.0 pmol); and (c) injection of AG1478 (1.0 pmol) into the rostral ventrolateral medulla. Values are expressed as mean ± SEM. $^{*}P < 0.05$; $^{\#}P < 0.01$ (vs. WKY rats, $n = 5$ per injection).

receptor antagonist as well as the ErbB4 receptor antagonist into the RVLM increased arterial pressure, HR, and RSNA. These data suggest that NRG-1/ErbB signaling in the RVLM is involved in regulating resting blood pressure. The depressor response to NRG-1 was nearly completely blocked when both ErbB2 and ErbB4 receptor blockers were administered. We cannot exclude the possibility that the ErbB3 receptors might also be involved in the depressor response to NRG-1 because NRG-1 stimulation could induce ErbB2/ErbB3 heterodimer or ErbB3 homodimer formation. We did not examine the effect of ErbB3 inhibition because the ErbB3 receptor antagonist is commercially not available. However, the role of the ErbB3 receptor in the NRG-1-induced hypotensive response in the RVLM is probably not that strong based on the results obtained using ErbB2 and ErbB4 receptor antagonists. It has been reported that only NRG-1, ErbB2, and ErbB4 are present in synapse-rich regions [32]. It should be noted that it has also been reported that peripheral NRG-1 affects cardiomyocytes, leading to negative inotropic effects [19]. Our findings are evoked by the agents of their central effects because the amount of the agents used in the present study is very small and directly administered into the RVLM. In fact, we did not find blood pressure and HR changes when the same amount of agents was administered systemically in Wistar rats.

It is possible that synaptic function alteration in the RVLM might be involved in the NRG-1-induced hypotensive response. The depressor response to NRG-1 injection into the RVLM was attenuated by the blockade of the GABA-A receptors. This supports the hypothesis that NRG-1 in the RVLM increases GABA, the major inhibitory neurotransmitter, and releases and/or augments GABA-A receptor activity. The pressor response to L-glutamate, the major excitatory neurotransmitter, was also attenuated prior to the injection of NRG-1 into the RVLM. This suggests that *N*-methyl-D-aspartic acid (NMDA) and/or non-NMDA response to L-glutamate is attenuated by NRG-1 stimulation. Because the major neurotransmitters involved in regulating the activity of RVLM neurons include glutamate and GABA [18], alteration of synaptic transmission induced by L-glutamate and GABA is important for regulating SNA [17]. NRG-1 and ErbB receptors are extensively distributed in the brain, including the medulla, and they exist in neurons, glia, and oligodendrocytes [3]. Also, it has been reported that glutamate and GABA receptors colocalizes with ErbB receptors in postsynaptic lesions [6–9]. Several studies have shown that the NRG-1/ErbB pathway is involved in the regulation of postsynaptic glutamate receptor function and presynaptic release of GABA, although these functions have not been determined for the RVLM [11,12,33,34]. For example, NRG-1 significantly enhances the depolarization-induced release of GABA in hippocampal neurons [11] and inhibits NMDA receptor currents in prefrontal cortex neurons [12,33,34]. Determining whether the actions are presynaptic vs. postsynaptic is difficult. We did not address

Fig. 5

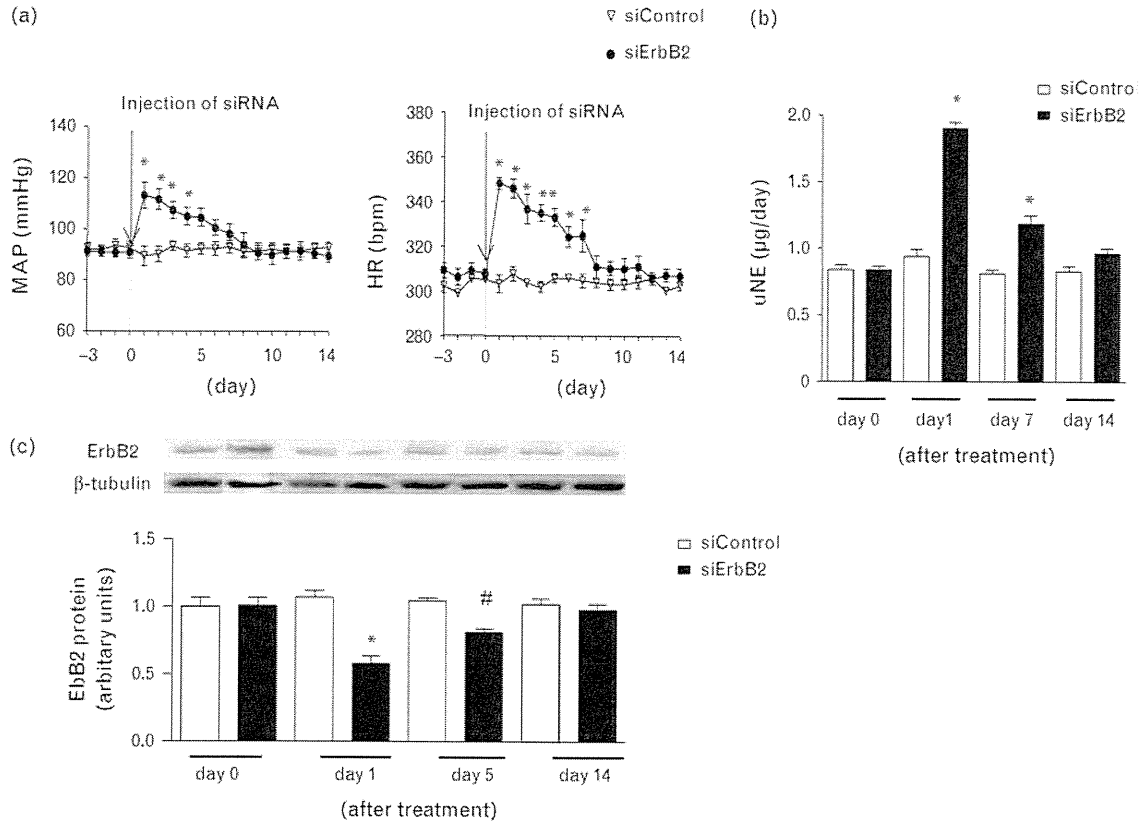

Effect of chronic ErbB2 receptor inhibition in the rostral ventrolateral medulla (RVLM) of Wistar–Kyoto rats on mean arterial pressure (MAP), heart rate (HR), and sympathetic nerve activity. (a) Effect of local administration of ErbB2 small-interference RNA (siRNA) (siErbB2) and control siRNA (siControl) into the RVLM on MAP and HR. $^{*}P < 0.05$ (vs. day-matched siControl treatment groups, $n = 5$ for each). (b) Group data for urinary norepinephrine excretion (uNE) at day 0 (before treatment), 1, 7, and 14 after starting the treatment (μg/day). $^{*}P < 0.01$ vs. siControl day 0 ($n = 5$ for each). (c) Western blot of ErbB2 in the RVLM in the siErbB2 treatment and siControl treatment groups. Western blot was performed at day 0 (before treatment), 1, 5, and 14 after starting the treatment. The densitometric average was normalized to the values obtained from the analysis of β-tubulin as internal control. $^{*}P < 0.01$; $^{\#}P < 0.05$ (vs. day0, $n = 5$ for each). Expressions are shown relative to that on day 0, which was assigned a value of 1. Values are expressed as mean ± SEM.

which cells were responsible for our observations. Further studies are necessary to clarify the precise mechanisms involved.

In addition to the blood pressure-lowering effect of the NRG-1/ErbB signaling in the RVLM through sympathoinhibition, we found that this signaling in the RVLM is impaired in SHRs compared with that in WKY rats. Particularly, reduced ErbB2 receptor expression levels in the RVLM of SHRs occurred during the prehypertensive age and persisted through the established hypertensive age of SHRs. Although NRG-1 and ErbB receptors are expressed in the brain, we did not observe reduced ErbB2 expression levels in other areas of the brain in SHRs (cerebral cortex and hypothalamus). Importantly, the depressor response to NRG-1 and the pressor response to the ErbB2 antagonist were attenuated in SHRs compared with responses in WKY rats. However, the pressor response to ErbB4 inhibitor did not differ between SHRs and WKY rats. Thus, we suggest that the reduction of ErbB2 receptors in the RVLM might contribute to the hypertensive state of SHRs.

On the basis of these findings, we further investigated whether a reduction in ErbB2 expression in the RVLM contributes to increased blood pressure in the conscious state. We inhibited ErbB2 expression in the RVLM of WKY rats using siRNAs. In this experiment, we used the AteloGene kit to deliver siErbB2 into the RVLM. AteloGene is a commercial kit used to locally administer siRNA into tissues *in vivo*. It has no toxicity and forms a gel in the body [35]. Thus, siRNA is maintained at the administration site [35]. Our findings indicate that reducing ErbB2 receptor expression levels in the RVLM increases blood pressure and HR and is associated with sympathoexcitation. These findings also suggest a dysfunction in NRG-1/ErbB signaling; reduction in ErbB2 levels in the RVLM might contribute to the neural mechanisms of hypertension in SHRs.

In conclusion, our findings indicate that the NRG-1/ErbB signaling in the RVLM exerts antihypertensive effects by reducing SNA in normotensive rats. Furthermore, impairment of NRG-1/ErbB signaling in the RVLM due to reduced levels of endogenous ErbB2 is a possible neural mechanism of hypertension in SHRs.

Acknowledgements

This study was supported by Grants-in-Aid for Scientific Research from the Japan Society for the Promotion of Science and a Grant from the Mitsubishi Pharma Research Foundation.

Conflicts of interest

There are no conflicts of interest.

References

1 Lemmens K, Doggen K, De Keulenaer GW. Role of neuregulin-1/ErbB signaling in cardiovascular physiology and disease: implications for therapy of heart failure. *Circulation* 2007; **116**:954–960.
2 Melenhorst WB, Mulder GM, Xi Q, Hoenderop JG, Kimura K, Eguchi S, van Goor H. Epidermal growth factor receptor signaling in the kidney: key roles in physiology and disease. *Hypertension* 2008; **52**:987–993.
3 Mei L, Xiong WC. Neuregulin 1 in neural development, synaptic plasticity and schizophrenia. *Nat Rev Neurosci* 2008; **9**:437–452.
4 Falls DL. Neuregulins: functions, forms, and signaling strategies. *Exp Cell Res* 2003; **284**:14–30.
5 Rio C, Rieff HI, Qi P, Khurana TS, Corfas G. Neuregulin and erbB receptors play a critical role in neuronal migration. *Neuron* 1997; **19**:39–50.
6 Gerecke KM, Wyss JM, Karavanova I, Buonanno A, Carroll SL. ErbB transmembrane tyrosine kinase receptors are differentially expressed throughout the adult rat central nervous system. *J Comp Neurol* 2001; **433**:86–100.
7 Thompson M, Lauderdale S, Webster MJ, Chong VZ, McClintock B, Saunders R, Weickert CS. Widespread expression of ErbB2, ErbB3 and ErbB4 in nonhuman primate brain. *Brain Res* 2007; **1139**:95–109.
8 Fox IJ, Kornblum HI. Developmental profile of ErbB receptors in murine central nervous system: implications for functional interactions. *J Neurosci Res* 2005; **79**:584–597.
9 Abe Y, Namba H, Zheng Y, Nawa H. In situ hybridization reveals developmental regulation of ErbB1-4 mRNA expression in mouse midbrain: implication of ErbB receptors for dopaminergic neurons. *Neuroscience* 2009; **161**:95–110.
10 Brinkmann BG, Agarwal A, Sereda MW, Garratt AN, Muller T, Wende H, *et al.* Neuregulin-1/ErbB signaling serves distinct functions in myelination of the peripheral and central nervous system. *Neuron* 2008; **59**:581–595.
11 Woo RS, Li XM, Tao Y, Carpenter-Hyland E, Huang YZ, Weber J, *et al.* Neuregulin-1 enhances depolarization-induced GABA release. *Neuron* 2007; **54**:599–610.
12 Li B, Woo RS, Mei L, Malinow R. The neuregulin-1 receptor erbB4 controls glutamatergic synapse maturation and plasticity. *Neuron* 2007; **54**:583–597.
13 Schmid RS, McGrath B, Berechid BE, Boyles B, Marchionni M, Sestan N, Anton ES. Neuregulin 1-erbB2 signaling is required for the establishment of radial glia and their transformation into astrocytes in cerebral cortex. *Proc Natl Acad Sci U S A* 2003; **100**:4251–4256.
14 Campos RR, Bergamaschi CT. Neurotransmission alterations in central cardiovascular control in experimental hypertension. *Curr Hypertens Rev* 2006; **2**:193–198.
15 Guyenet PG. The sympathetic control of blood pressure. *Nat Rev Neurosci* 2006; **7**:335–346.
16 Hirooka Y, Sagara Y, Kishi T, Sunagawa K. Oxidative stress and central cardiovascular regulation. *Circ J* 2010; **74**:827–835.
17 Sved AF, Ito S, Sved JC. Brainstem mechanisms of hypertension: role of the rostral ventrolateral medulla. *Curr Hypertens Rep* 2003; **5**:262–268.
18 Schreihofer AM, Guyenet PG. The baroreflex and beyond: control of sympathetic vasomotor tone by GABAergic neurons in the ventrolateral medulla. *Clin Exp Pharmacol Physiol* 2002; **29**:514–521.
19 Lemmens K, Fransen P, Sys SU, Brutsaert DL, De Keulenaer GW. Neuregulin-1 induces a negative inotropic effect in cardiac muscle: role of nitric oxide synthase. *Circulation* 2004; **109**:324–326.
20 Zhu WZ, Xie Y, Moyes KW, Gold JD, Askari B, Laflamme MA. Neuregulin/ErbB signaling regulates cardiac subtype specification in differentiating human embryonic stem cells. *Circ Res* 2010; **107**:776–786.
21 Tsai CM, Levitzki A, Wu LH, Chang KT, Cheng CC, Gazit A, Perng RP. Enhancement of chemosensitivity by tyrphostin AG825 in high-p185(neu) expressing nonsmall cell lung cancer cells. *Cancer Res* 1996; **56**:1068–1074.
22 Osherov N, Gazit A, Gilon C, Levitzki A. Selective inhibition of the epidermal growth factor and HER2/neu receptors by tyrphostins. *J Biol Chem* 1993; **268**:11134–11142.
23 Ishii Y, Fujimoto S, Fukuda T. Gefitinib prevents bleomycin-induced lung fibrosis in mice. *Am J Respir Crit Care Med* 2006; **174**:550–556.
24 Gajendran N, Kapfhammer JP, Lain E, Canepari M, Vogt K, Wisden W, Brenner HR. Neuregulin signaling is dispensable for NMDA- and GABA(A)-receptor expression in the cerebellum in vivo. *J Neurosci* 2009; **29**:2404–2413.
25 Choi BH, Choi JS, Rhie DJ, Yoon SH, Min DS, Jo YH, *et al.* Direct inhibition of the cloned Kv1.5 channel by AG-1478, a tyrosine kinase inhibitor. *Am J Physiol Cell Physiol* 2002; **282**:C1461–C1468.
26 Kishi T, Hirooka Y, Sakai K, Shigematsu H, Shimokawa H, Takeshita A. Overexpression of eNOS in the RVLM causes hypotension and bradycardia via GABA release. *Hypertension* 2001; **38**:896–901.
27 Hirooka Y, Polson JW, Dampney RA. Pressor and sympathoexcitatory effects of nitric oxide in the rostral ventrolateral medulla. *J Hypertens* 1996; **14**:1317–1324.
28 Horiuchi J, Dampney RA. Evidence for tonic disinhibition of RVLM sympathoexcitatory neurons from the caudal pressor area. *Auton Neurosci* 2002; **99**:102–110.
29 Kishi T, Hirooka Y, Kimura Y, Ito K, Shimokawa H, Takeshita A. Increased reactive oxygen species in rostral ventrolateral medulla contribute to neural mechanisms of hypertension in stroke-prone spontaneously hypertensive rats. *Circulation* 2004; **109**:2357–2362.
30 Grazette LP, Boecker W, Matsui T, Semigran M, Force TL, Hajjar RJ, Rosenzweig A. Inhibition of ErbB2 causes mitochondrial dysfunction in cardiomyocytes: implications for herceptin-induced cardiomyopathy. *J Am Coll Cardiol* 2004; **44**:2231–2238.
31 Sakai K, Hirooka Y, Matsuo I, Eshima K, Shigematsu H, Shimokawa H, Takeshita A. Overexpression of eNOS in NTS causes hypotension and bradycardia in vivo. *Hypertension* 2000; **36**:1023–1028.
32 Chaudhury AR, Gerecke KM, Wyss JM, Morgan DG, Gordon MN, Carroll SL. Neuregulin-1 and erbB4 immunoreactivity is associated with neuritic plaques in Alzheimer disease brain and in a transgenic model of Alzheimer disease. *J Neuropathol Exp Neurol* 2003; **62**:42–54.
33 Gu Z, Jiang Q, Fu AK, Ip NY, Yan Z. Regulation of NMDA receptors by neuregulin signaling in prefrontal cortex. *J Neurosci* 2005; **25**:4974–4984.
34 Fischbach GD. NRG1 and synaptic function in the CNS. *Neuron* 2007; **54**:495–497.
35 Minakuchi Y, Takeshita F, Kosaka N, Sasaki H, Yamamoto Y, Kouno M, *et al.* Atelocollagen-mediated synthetic small interfering RNA delivery for effective gene silencing in vitro and in vivo. *Nucleic Acids Res* 2004; **32**:e109.

Clinical and Experimental Hypertension, 33(4):240–245, (2011)

ISSN 1064-1963 print/1525-6006 online
DOI: 10.3109/10641963.2011.583969

informa
healthcare

Calorie Restriction inhibits Sympathetic Nerve Activity via Anti-Oxidant Effect in the Rostral Ventrolateral Medulla of Obesity-Induced Hypertensive Rats

Takuya Kishi, Yoshitaka Hirooka, Kiyohiro Ogawa, Satomi Konno, Kenji Sunagawa

Department of Advanced Therapeutics for Cardiovascular Diseases, Department of Cardiovascular Medicine, Kyushu University Graduate School of Medical Sciences, Fukuoka, Japan

Abstract

In the patients and animals with metabolic syndrome (MetS), sympathetic nerve activity (SNA) is increased. We have demonstrated that oxidative stress in the rostral ventrolateral medulla (RVLM), a vasomotor center in the brainstem, increases SNA. The aim of the present study was to determine whether calorie restriction inhibits SNA via anti-oxidant effect in the RVLM of obesity-induced obesity rats. Male Sprague-Dawley rats were fed on a high-fat diet and segregated into obesity-prone (OP) showing a MetS profile and obesity-resistant (OR) after 13 weeks. Obesity-prone was divided into OP treated with calorie restriction (CR-OP) for 8 weeks and control (CTR-OP). Systolic blood pressure (SBP), heart rate (HR), SNA, and thiobarbituric acid-reactive substances (TBARS) levels as a marker of oxidative stress in the RVLM were significantly higher and the depressor effects due to the microinjection of tempol, a superoxide dismutase mimetic into the RVLM, were significantly greater in OP than in OR. Body weight was significantly lower in CR-OP than in CTR-OP. SBP, HR, SNA, TBARS, and the depressor effects due to the microinjection of tempol into the RVLM were significantly lower in CR-OP than in CTR-OP. These results suggest that calorie restriction inhibits SNA via anti-oxidant effect in the RVLM of obesity-induced obesity rats.

keywords: calorie restriction, metabolic syndrome, sympathetic nerve activity, oxidative stress, brain

INTRODUCTION

Metabolic syndrome (MetS), a complex of highly debilitating disorders that consist of hypertension, diabetes mellitus, and dyslipidemia, is associated with the development of visceral obesity (1). Previous study indicated that sympathetic activation may be involved in obesity-induced hypertension (2). In obesity-induced hypertension, increased oxidative stress in the hypothalamus may contribute to the progression of hypertension through central sympatho-excitation (3). Several studies have also suggested that oxidative stress may be the unifying mechanisms underlying the development of hypertension in obesity (4–6). In preclinical testing, one non-pharmacologic approach that was shown to be beneficial in a variety of cardiovascular diseases is long-term calorie restriction (CR) (7–9). Although long-term CR has been shown to prevent increases in blood pressure (BP) in nonobese hypertensive rats, little is known about the mechanisms responsible for these observations.

Rostral ventrolateral medulla (RVLM) in the brainstem is the vasomotor center that determines basal sympathetic nerve activity (SNA), and the functional integrity of the RVLM is essential for the maintenance of basal vasomotor tone (10, 11). We have demonstrated that oxidative stress in the RVLM produced by angiotensin II type 1 receptor (AT_1R) increases the SNA (12, 13), and that nitric oxide (NO) in the RVLM decreases the SNA (14–17). Our other reports have suggested that the imbalance between oxidative stress and NO in the brain cause cardiovascular diseases (18–22). Previous reports have suggested that oxidative stress in the hypothalamus cause sympatho-excitation in the obesity-induced hypertensive rats (3), and that neurons in the RVLM contribute to elevated sympathetic outflow in a rodent model of diet-induced obesity (23). However, it has not been determined whether the calorie restriction decreases SNA via anti-oxidant in the RVLM of obesity-induced hypertensive rats.

Address correspondence to Takuya Kishi, MD, PhD, FAHA, Department of Advanced Therapeutics for Cardiovascular Diseases, Department of Cardiovascular Medicine, Kyushu University Graduate School of Medical Sciences, 3-1-1 Maidashi, Higashi-ku, Fukuoka 812-8582, Japan. E-mail: tkishi@cardiol.med.kyushu-u.ac.jp

Received 31 August 2010; revised 9 November 2010; accepted 12 November 2010.

Therefore, the aim of the present study was to investigate the effect of calorie restriction on the SNA and oxidative stress in the RVLM of obesity-induced hypertensive rats. To determine this aim, we measured BP, heart rate (HR), urine norepinephrine excretion as a parameter of SNA, and oxidative stress in the RVLM. Furthermore, to inhibit the oxidative stress in the RVLM locally, we microinjected tempol, a superoxide dismutase (SOD) mimetic, into the RVLM. Previously, we performed the same experiments in the hypertensive model rats, in which the microinjection of tempol into the RVLM caused depressor and bradycardia (12). In that experiment, we also performed the overexpression of Mn-SOD into the bilateral RVLM of hypertensive rats, and inhibited the oxidative stress in the RVLM locally. The overexpression of Mn-SOD in the RVLM caused the sympatho-inhibition, and the depressor and bradycardiac responses were similar to those effects caused by the microinjection of tempol into the RVLM. We consider that microinjection of tempol into the RVLM locally causes the sympatho-inhibition due to the reduction of oxidative stress in the RVLM locally. Furthermore, to increase the oxidative stress in the RVLM, we microinjected angiotensin II into the RVLM of OP, OR, CTR-OP, and CR-OP. Previously, we performed the same experiments in the hypertensive model rats, in which the microinjection of angiotensin II into the RVLM increased sympathetic nerve activity due to the increase in oxidative stress in the RVLM (20).

MATERIALS AND METHODS

Animals

This study was reviewed and approved by the Committee on Ethics of Animal Experiments, Kyushu University Graduate School of Medical Sciences, and conducted according to the Guidelines for Animal Experiments of Kyushu University. Male Sprague-Dawley rats (Charles River Laboratories, Kingston, NY) weighing between 350 to 425 g were housed individually in a temperature-controlled room (22° to 23°C) with a 12-h/12-h light-dark cycle (lights on at 7:00 AM). Rats were placed on a moderate high-fat diet (32% kcal from fat, Research Diets, New Brunswick, NJ) for 13 weeks. After 5 weeks, rats fed the moderately high-fat diet segregate into obesity prone (OP) and obesity resistance (OR) based on the body weight distribution as described previously (23). Briefly, a body weight histogram was constructed and resulted in a distribution of rats into OP and OR groups corresponding with the upper and lower one-third of rats, respectively.

Calorie Restriction

Obesity prone rats in the calorie restriction (CR-OP) group were given 70% of their mean 24-h food intake. Food was given to the CR-OP group daily 2–3 h before lights off. The restricted feeding was continued for 8 weeks (24). Obesity prone rats in the control (CTR-OP) group were free to have food.

Measurement of BP, HR, and SNA

Systolic blood pressure (SBP) and HR were measured using the tail-cuff method (BP-98A; Softron, Tokyo, Japan). We calculated the urinary norepinephrine excretion for 24 h as an indicator of SNA, as described previously (12, 14).

Measurement of TBARS

To obtain the RVLM tissues, the rats were deeply anesthetized with sodium pentobarbital (100 mg/kg IP) and perfused transcardially with PBS (150 mol/L NaCl, 3 mmol/L KCl, and 5 nmol/L phosphate; pH 7.4, 4°C). The brains were removed quickly, and sections 1 mm thick were obtained with a cryostat at -7 ± 1°C. The RVLM was defined according to a rat brain atlas as described previously (12), and obtained by a punch-out technique. The RVLM tissues were homogenized in 1.15% KCl (pH 7.4) and 0.4% sodium dodecyl sulfate, 7.5% acetic acid adjusted to pH 3.5 with NaOH. Thiobarbituric acid (0.3%) was added to the homogenate. The mixture was maintained at 5°C for 60 min, followed by heating to 100°C for 60 min. After cooling, the mixture was extracted with distilled water and *n*-butanolpyridine (15:1) and centrifuged at 1600*g* for 10 min. The absorbance of the organic phase was measured at 532 nm. The amount of thiobarbituric acid-reactive substances (TBARS) was determined by absorbance, as described previously (12).

Microinjection of Tempol and Angiotensin II into the RVLM

To inhibit the oxidative stress in the RVLM, we microinjected tempol (1 nmol) into the RVLM of OP, OR, CTR-OP, and CR-OP which were anesthetized with sodium pentobarbital , as described previously (12). One h after the microinjection of tempol, we determined the recovery of BP and HR to the levels of baseline, and we microinjected angiotensin II (50 pmol) into the RVLM. A catheter was inserted into the femoral artery to record arterial BP. A tracheal cannula was connected to a ventilator, and the rats were artificially ventilated. The rats were placed in a stereotaxic frame. A glass micropipette was filled with tempol, angiotensin II, or L-glutamate and positioned at the injection site. Before the microinjection, the RVLM was identified by monitoring the mean arterial pressure (MAP) after injection of a small dose of L-glutamate. The identification of the RVLM was confirmed as described previously (12).

Statistical Analysis

All values are expressed as mean ± SEM. Comparisons between any two mean values were performed using Bonferroni's correction for multiple comparisons. ANOVA was used to compare the body weight, blood pressure, and TBARS levels in CR-OP or CTR-OP.

Differences were considered to be statistically significant at a P value of <0.05.

RESULTS

Body Weight, BP, HR, Urinary Norepinephrine Excretion, and TBARS levels in the RVLM before CR

Before the start of the CR, OP rats weighed significantly more than OR (Figure 1). Systolic BP and HR were also significantly higher in OP than in OR (Figures 2A and 2B). The peak of the depressor and bradycardiac responses due to the microinjection of tempol into the RVLM was around 10 min after the injection, and the responses were significantly greater in OP than OR (-24 ± 4 mmHg vs. -7 ± 5 mmHg, -30 ± 6 bpm vs. -4 ± 3 bpm, n = 4 for each, P < 0.05 for each, Figure 3A). The peak of the presser and tachycardic responses due to the microinjection of angiotensin II into the RVLM was around 15 min after the injection, and the responses were significantly greater in OP than in OR (Figure 3B). Urinary norepinephrine excretion was significantly higher in OP than in OR (Figure 4A). TBARS levels in the RVLM were significantly higher in OP than in OR (Figure 4B).

Body Weight, BP, HR, Urinary Norepinephrine Excretion, and TBARS levels in the RVLM after CR

Eight weeks after the CR, CR-OP rats weighed significantly less than CTR-OP and OP before CR (Figure 1). Systolic blood pressure and HR were also significantly lower in CR-OP than in CTR-OP and in OP before CR (Figures 2A and 2B). The depressor effects and bradycardia due to the microinjection of tempol into the RVLM were significantly smaller in CR-OP than in CTR-OP (-14 ± 3 mmHg vs. -28 ± 4 mmHg, -11 ± 6 bpm vs. -38 ± 4 bpm, n = 4 for each, P < 0.05 for each, Figure 3A). The pressor effects and tachycardia due to the microinjection of angiotensin II into the RVLM were significantly smaller in CR-OP than in CTR-OP (Figure 3B). Urinary norepinephrine excretion was significantly lower in CR-OP than in CTR-OP and in OP before CR (Figure 4A). TBARS levels in the RVLM were significantly lower in CR-OP than in CTR-OP and in OP before CR (Figure 4B).

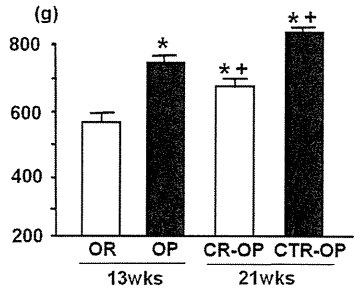

Figure 1. Body weights of OP and OR before calorie restriction, and CR-OP and CTR-OP after calorie restrictions for 8 weeks. Data are shown as mean ± SEM (n = 5 for each group). *P < 0.05 vs. OR; +P < 0.05 vs. OP.

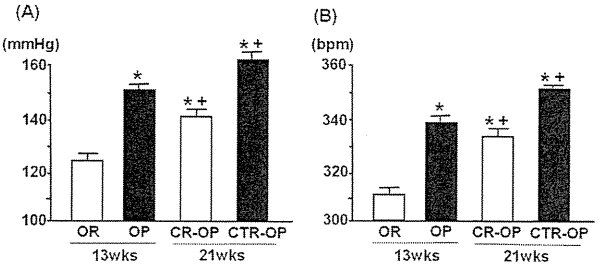

Figure 2. **(A)** Systolic blood pressure of OP and OR before calorie restriction, and CR-OP and CTR-OP after calorie restriction for 8 weeks. Data are shown as mean ± SEM (n =5 for each group). *P < 0.05 vs. OR; +P < 0.05 vs. OP. **(B)** Heart rate of OP and OR before calorie restriction, and CR-OP and CTR-OP after calorie restriction for 8 weeks. Data are shown as mean ± SEM (n = 5 for each group). *P < 0.05 vs. OR; +P < 0.05 vs. OP.

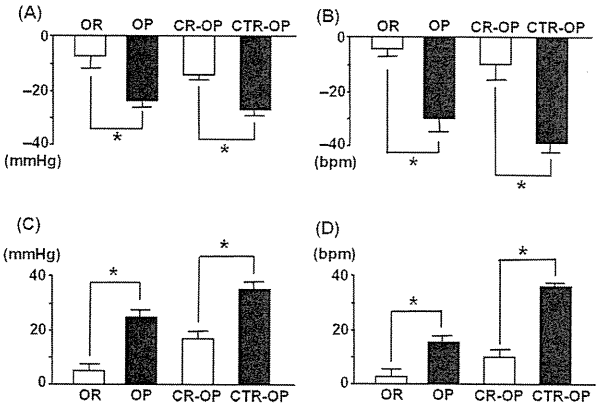

Figure 3. **(A)** Changes in mean BP due to the microinjection of tempol into the RVLM of OP, OR, CR-OP, and CTR-OP. Data are shown as mean ± SEM (n = 4 for each group). *P < 0.05. **(B)** Changes in HR due to the microinjection of tempol into the RVLM of OP, OR, CR-OP, and CTR-OP. Data are shown as mean ± SEM (n = 4 for each group). *P < 0.05. **(C)** Changes in mean BP due to the microinjection of angiotensin II into the RVLM of OP, OR, CR-OP, and CTR-OP. Data are shown as mean ± SEM (n = 4 for each group). *P < 0.05. **(D)** Changes in HR due to the microinjection of angiotensin II into the RVLM of OP, OR, CR-OP, and CTR-OP. Data are shown as mean ± SEM (n = 4 for each group). *P < 0.05.

DISCUSSION

In the present study, we have demonstrated three findings for the first time. First, in obesity-induced hypertensive rats, oxidative stress in the RVLM was increased. Second, calorie restriction decreased sympathetic nerve activity and oxidative stress in obesity-induced hypertensive rats. Third, the depressor and bradycardic response caused by the inhibition of oxidative stress in the RVLM locally were significantly smaller in calorie-restricted obesity rats than in control-obesity rats. These results suggest that obesity enhances oxidative stress in the RVLM, which causes sympatho-excitation and

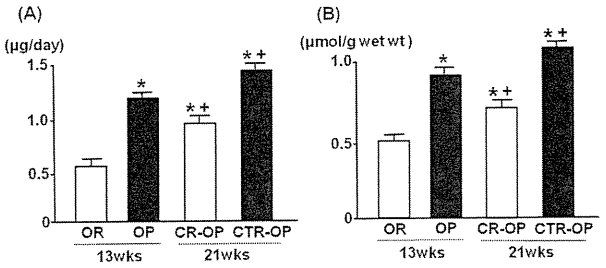

Figure 4. **(A)** Twenty-four hour norepinephrine excretions per body weights of OP and OR before calorie restriction, and CR-OP and CTR-OP after calorie restriction for 8 weeks. Data are shown as mean ± SEM (n = 5 for each group). *P < 0.05 vs. OR; +P < 0.05 vs. OP. **(B)** TBARS levels in the RVLM of OP and OR before calorie restriction, and CR-OP and CTR-OP after calorie restriction for 8 weeks. Data are shown as mean ± SEM (n = 5 for each group). *P < 0.05 vs. OR; +P < 0.05 vs. OP.

hypertension, and that calorie restriction reduces not only body weight but also SNA, probably due to the anti-oxidant in the RVLM.

In the present study, we demonstrated that oxidative stress in the RVLM is increased in obesity-induced hypertensive rat, and that the depressor and bradycardic response caused by the inhibition of oxidative stress in the RVLM locally due to the microinjection of tempol were significantly greater in obesity-induced hypertensive rats than in obesity-resistance rats. Several reports suggest that oxidative stress in the kidney (4), heart (5), and arteries (4, 5) is involved in obesity-induced hypertension. In the brain, high dietary fat has been reported to induce oxidative stress and inflammation in the brain (25), and other previous report have suggested that oxidative stress in the hypothalamus is increased, which cause sympatho-excitation in obesity-induced hypertensive rats (3). Although the RVLM is a vasomotor center and oxidative stress in the RVLM is the most major sympatho-exciting factor, this is the first study examining the oxidative stress in the RVLM of obesity-induced hypertensive rats. However, the mechanisms in which obesity increase oxidative stress in the RVLM have not been conclusive in the present study. Several studies have shown that the central renin-angiotensin system mediates oxidative stress (26, 27), and it is well known that adipose tissue can secrete angiotensinogen (28). In the present study, we demonstrated that the microinjection of angiotensin II into the RVLM caused presser response and tachycardia, and that the effects were significantly greater in OP than in OR, and were significantly smaller in CR-OP than in CTR-OP. Furthermore, rats fed a high fructose diet, a model of insulin resistance, have an increased oxidative stress (29). A peroxisome proliferator-activated receptor-gamma agonist, which ameliorates insulin resistance, prevented hypertension and oxidative stress in dietary-induced obesity rats (30). In addition, there is a possibility that leptin, a polypeptide hormone mediator produced by adipocytes, stimulates oxidative stress generation in the brain (31). We consider that the increase in oxidative stress in the RVLM through the renin-angiotensin system is the most important factor in the obesity-induced hypertension, because oxidative stress in the RVLM is the most major sympatho-exciting factor (12).

Moreover, in the present study, we also demonstrated that calorie restriction inhibits oxidative stress in the RVLM of obesity-induced hypertensive rats, and that the depressor and bradycardic response caused by the inhibition of oxidative stress in the RVLM locally were significantly smaller in calorie-restricted obesity rats than in control-obesity rats. This reduction of oxidative stress in the RVLM might cause sympatho-inhibition. This is the first study which demonstrates that calorie restriction inhibits oxidative stress in the brain.

Although the mechanism in which calorie restriction inhibits oxidative stress in the brain could not been determined in the present study, we hypothesize that calorie restriction may improve adipocytes, inhibit central renin-angiotensin system, directly inhibit oxidative stress in the RVLM, and indirectly inhibit oxidative stress in the RVLM through the inhibition of oxidative stress in the hypothalamus. Circulating angiotensin II acts at circumventricular organs to subsequently activate complex pathways, including those using central angiotensin II as a neurotransmitter, to increases sympathetic outflow (32). However, it is necessary to do further examination.

There are some limitations in the present study. First, we only examined the oxidative stress in the RVLM. There are some important nuclei and areas involved in the cardiovascular control, such as nucleus tractus solitarii, hypothalamus, and so on. The increase in oxidative stress in the obesity-induced hypertension and the reduction of oxidative stress due to calorie restriction may not be the unique phenomenon in the RVLM. From this reason, in the present study, we examined only TBARS methods for the RVLM tissues obtained by the punch-out method, not the histologic examination. However, in the regulation of sympathetic nerve activity, RVLM is the most important cite. Furthermore, in the RVLM, oxidative stress is the most powerful and important sympatho-exciting factor. In the present study, we focused on the oxidative stress in the RVLM of obesity-induced hypertensive rats. Second, in the present study, we could not check the renin-angiotensin system in the RVLM. In the RVLM, oxidative stress is generated by AT_1R and NAD (P) H oxidase. We have the speculation that AT_1R and NAD (P) H oxidase in the RVLM may be activated in the obesity-induced hypertension, and that calorie restriction inhibits AT_1R and NAD (P) H oxidase in the RVLM. We have to perform further studies.

CONCLUSIONS

Our results suggest that, in obesity-induced hypertensive rats, oxidative stress in the RVLM is increased,

and that calorie restriction decreases sympathetic nerve activity through the anti-oxidant in the RVLM of obesity-induced hypertensive rats. These results suggest that obesity enhances oxidative stress in the RVLM, which causes sympatho-excitation and hypertension, and that calorie restriction reduces not only body weight but also sympathetic nerve activity, probably due to the anti-oxidant in the RVLM.

ACKNOWLEDGMENTS

This study was supported by a grant-in-aid for scientific research from the Japan Society for the Promotion of Science (B19390231) and, in part, by the Health and Labor Sciences Research Grant for Comprehensive Research in Aging and Health Labor and Welfare of Japan. We express thanks to Satomi and Jiro.

Declaration of interest: The authors report no conflicts of interest. The authors alone are responsible for the content and writing of the papers.

REFERENCES

[1] Dandona P, Aljada A, Chaudhuri A, Mohanty P, Garg R. Metabolic syndrome: a comprehensive perspective based on interactions betweenobesity, diabetes, and inflammation. *Circulation* 2005;111:1448–1454.

[2] Esler M, Straznicky N, Eikelis N, Masuo K, Lambert G, Lambert E. Mechanisms of sympathetic activation in obesity-related hypertension. *Hypertension* 2006;48:787–796.

[3] Nagae A, Fujita M, Kawarazaki H, Matsui H, Ando K, Fujita T. Sympathoexcitation by oxidative stress in the brain mediates arterial pressure elevation in obesity-induced hypertension. *Circulation* 2009;119:978–986.

[4] Dobrian AD, Davies MJ, Schriver SD, Lauterio TJ, Prewitt RL. Oxidative stress in a rat model of obesity-induced hypertension. *Hypertension* 2001;37:554–560.

[5] Matsui H, Ando K, Kawarazaki H, Nagae A, Fujita M, Shimosawa T, Nagase M, Fujita T. Salt excess causes left ventricular diastolic dysfunction in rats with metabolic disorder. *Hypertension* 2008;52:287–294.

[6] Smith AD, Brands MW, Wang MH, Dorrance AM. Obesity-induced hypertension develops in young rats independently of the renin-angiotensin-aldosterone system. *Exp Biol Med (Maywood)* 2006;231:282–287.

[7] Holloszy JO, Fontana L. Caloric restriction in humans. *Exp Gerontol* 2007;42:709–712.

[8] Pedrozo H, Bertrand HA, Herlihy JT. Caloric restriction alters arterialblood pressure and baroreflex responsiveness of the SHR. *Age* 1994;17:23–27.

[9] Young JB, Mullen D, Landsberg L. Caloric restriction lowers bloodpressure in the SHR. *Metab Clin Exp* 1978;27:1711–1714.

[10] Dampney RA. Functional organization of central pathways regulating the cardiovascular system. *Physiol Rev* 1994;74:323–364.

[11] Guyenet PG. The sympathetic control of blood pressure. *Nat Rev Neurosci* 2006;7:335–346.

[12] Kishi T, Hirooka Y, Kimura Y, Ito K, Shimokawa H, Takeshita A. Increased reactive oxygen species in rostral ventrolateral medulla contribute to neural mechanisms of hypertension in stroke-prone spontaneously hypertensive rats. *Circulation* 2004;109:3257–3262.

[13] Kishi T, Hirooka Y, Konno S, Ogawa K, Sunagawa K. Angiotensin II type 1 receptor-activated caspase-3 through ras/mitogen-activated protein kinase/extracellular signal-regulated kinase in the rostral ventrolateral medulla is involved in sympathoexcitation in stroke-prone spontaneously hypertensive rats. *Hypertension* 2010;55:291–297.

[14] Kishi T, Hirooka Y, Sakai K, Shigematsu H, Shimokawa H, Takeshita A. Overexpression of eNOS in the RVLM causes hypotension and bradycardia via GABA release. *Hypertension* 2001;38:896–901.

[15] Hirooka Y, Sakai K, Kishi T, Takeshita A. Adenovirus-mediated gene transfer into the NTS in conscious rats. A new approach to examining the central control of cardiovascular regulation. *Ann N Y Acad Sci* 2001;940:197–205.

[16] Hirooka Y, Kishi T, Sakai K, Shimokawa H, Takeshita A. Effect of overproduction of nitric oxide in the brain stem on the cardiovascular response in conscious rats. *J Cardiovasc Pharmacol* 2003;41:S119–S126.

[17] Hirooka Y, Shigematsu H, Kishi T, Kimura Y, Ueta Y, Takeshita A. Reduced nitric oxide synthase in the brainstem contributes to enhanced sympathetic drive in rats with heart failure. *J Cardiovasc Pharmacol* 2003;42:S111–S115.

[18] Sakai K, Hirooka Y, Shigematsu H, Kishi T, Ito K, Shimokawa H, Takeshita A, Sunagawa K. Overexpression of eNOS in brain stem reduces enhanced sympathetic drive in mice with myocardial infarction. *Am J Physiol* 2005;289:H2159–H2166.

[19] Nozoe M, Hirooka Y, Koga Y, Sagara Y, Kishi T, Engelhardt JF, Sunagawa K. Inhibition of Rac1-derived reactive oxygen species in nucleus tractus solitarius decreases blood pressure and heart rate in stroke-prone spontaneously hypertensive rats. *Hypertension* 2007;50:62–68.

[20] Nozoe M, Hirooka Y, Koga Y, Araki S, Konno S, Kishi T, Ide T, Sunagawa K. Mitochondria-derived reactive oxygen species mediate sympathoexcitation induced by angiotensin II in the rostral ventrolateral medulla. *J Hypertens* 2008;26:2176–2184.

[21] Kishi T, Hirooka Y, Shimokawa H, Takeshita A, Sunagawa K. Atorvastatin reduces oxidative stress in the rostral ventrolateral medulla in stroke-prone spontaneously hypertensive rats. *Clin Exp Hypertens* 2008;30:1–9.

[22] Kishi T, Hirooka Y, Ito K, Sakai K, Shimokawa H, Takeshita A. Cardivascular effects of overexpression of endothelial nitric oxide synthase in the rostral ventrolateral medulla in stroke-prone spontaneously hypertensive rats. *Hypertension* 2002;39:264–268.

[23] Stocker SD, Meador R, Adams JM. Neurons of the rostral ventrolateral medulla contribute to obesity-induced hypertension in rats. *Hypertension* 2007;49:640–646.

[24] Teske JA, Kotz CM. Effect of acute and chronic calonic restriction and metabolic glucoprivation on spontaneous physical activity in obesity-prone and obesity-resistance rats. *Am J Physiol* 2009;297:R176–R184.

[25] Zhang X, Dong X, Ren J, Driscoll MJ, Culver B. High dietary fat induces NADPH oxidase-associated oxidative stress and inflammation in rat cerebral cortex. *Exp Neurol* 2005;191:318–325.

[26] Zimmerman MC, Lazartigues E, Sharma RV, Davisson RL. Hypertension caused by angiotensin II infusion involves increased superoxide production in the central nervous system. *Circ Res* 2004;95:210–216.

[27] Zimmerman MC, Lazartigues E, Lang JA, Sinnayah P, Ahmad IM, Spitz DR, Davisson RL. Superoxide mediates the actions of angiotensin II inthe central nervous system. *Circ Res* 2002;91:1038–1045.

[28] Boustany CM, Bharadwaj K, Daugherty A, Brown DR, Randall DC, Cassis LA. Activation of the systemic and adipose renin-angiotensin system in rats with diet-induced obesity and hypertension. *Am J Physiol* 2004;287:R943–R949.

[29] Delbosc S, Paizanis E, Magous R, Araiz C, Dimo T, Cristol JP, Cros G, Azay J. Involvement of oxidative stress and NADPH

oxidase activation in the development of cardiovascular complications in a model of insulin resistance, the fructose-fed rat. *Atherosclerosis* 2005;179:43–49.

[30] Dobrian AD, Schriver SD, Khraibi AA, Prewitt RL. Pioglitazone prevents hypertension and reduces oxidative stress in diet-induced obesity. *Hypertension* 2004;43:48–56.

[31] Lauterio TJ, Davies MJ, DeAngelo M, Peyser M, Lee J. Neuropeptide Y expression and endogenous leptin concentrations in a dietary model of obesity. *Obes Res* 1999;7:498–505.

[32] Ferguson AV, Washburn DL. Angiotensin II: a peptidergic neurotransmitter in central autonomic pathways. *Prog Neurobiol* 1998;54:169–192.

Clinical and Experimental Hypertension, 33(4):223–230, (2011)

ISSN 1064-1963 print/1525-6006 online
DOI: 10.3109/10641963.2011.583967

informa
healthcare

Role of Angiotensin-(1-7) in Rostral Ventrolateral Medulla in Blood Pressure Regulation via Sympathetic Nerve Activity in Wistar-Kyoto and Spontaneous Hypertensive Rats

Toshiaki Nakagaki,[1,2] Yoshitaka Hirooka,[1] Koji Ito,[1] Takuya Kishi,[1] Sumio Hoka,[2] Kenji Sunagawa[1]

[1]*Department of Cardiovascular Medicine, Kyushu University Graduate School of Medical Sciences, Fukuoka, Japan,* [2]*Department of Anesthesiology and Critical Care Medicine, Kyushu University Graduate School of Medical Sciences, Fukuoka, Japan*

Abstract

Angiotensin (Ang)-(1-7) Ang-(1-7) is formed from angiotensin II by angiotensin-converting enzyme 2 (ACE2) and modulates the renin-angiotensin system. We evaluated whether the Ang-(1-7)-Mas axis in the rostral ventrolateral medulla (RVLM) contributes to neural mechanisms of blood pressure (BP) regulation. We microinjected Ang-(1-7), Ang-(1-7)-Mas receptor antagonist A-779, and ACE2 inhibitor DX600 into the RVLM of anesthetized Wistar-Kyoto rats (WKY) and spontaneously hypertensive rats (SHRs). Unilateral Ang-(1-7) microinjection induced a significantly greater increase in AP (arterial blood pressure) in SHR than in WKY. Bilateral A-779 microinjection induced a significantly greater decrease in AP and renal sympathetic nerve activity in SHR than in WKY. Bilateral DX600 microinjection induced a significantly greater decrease in AP in SHR than in WKY. Our results suggest that endogenous Ang-(1-7) in the RVLM contributes to maintain AP and renal sympathetic nerve activity both in SHR and WKY and that its activity might be enhanced in SHR.

keywords: angiotensin-(1-7), blood pressure, sympathetic nervous system, rostral ventrolateral medulla, hypertension

INTRODUCTION

Accumulating evidence indicates that the sympathetic nervous system plays an important role in the pathogenesis of hypertension (1–3). It is well established that the renin-angiotensin system (RAS) modulates blood pressure (BP) (4). The RAS members may act as neuromodulators in different sites of the brain, and dysfunction in the brain RAS is implicated in the pathogenesis of hypertension (5). The rostral ventrolateral medulla (RVLM) is the major vasomotor center that determines basal sympathetic nervous system activity and is essential for the maintenance of basal vasomotor tone (6). Activation of angiotensin type 1 (AT_1) receptors in the RVLM evokes sympathetic excitation and pressor effects in normal animals (7,8) and appears to be important for the maintenance of hypertension in spontaneously hypertensive rats (SHR) (9).

Angiotensin-(1-7) [Ang-(1-7)] is a biologically active peptide of the RAS family. It is formed from angiotensin (Ang) I or II by an angiotensin-converting enzyme homolog (ACE2) (10). The action of Ang-(1-7) is mediated through its selective receptor Mas (11), which is different from AT_1 or AT_2 receptor subtypes, and is blocked by its specific antagonist A-779. Ang-(1-7) is active in central areas of cardiovascular control, including neurons in the nucleus tractus solitarius (NTS) (12), RVLM (13,14), and paraventricular nucleus (PVN) (15). The Mas receptor and ACE2 are present in different areas related to cardiovascular control in the brain (16,17). Although Ang II and Ang-(1-7) have opposite effects systemically, microinjection of Ang-(1-7) or Ang-II into the RVLM elicits a similar pressor response (18,19).

The objective of the present study was to determine whether Ang-(1-7) in the RVLM contributes to the maintenance or elevation of BP in a rat model of hypertension. Therefore, we investigated the cardiovascular effects of microinjection of Ang-(1-7), its selective antagonist A-779, and the ACE2 inhibitor DX600 into the RVLM in normotensive and hypertensive rats.

Address correspondence to Yoshitaka Hirooka, MD, PhD, FAHA, Department of Cardiovascular Medicine, Kyushu University Graduate School of Medical Sciences, 3-1-1 Maidashi, Higashi-ku, Fukuoka, 812-8582, Japan. E-mail: hyoshi@cardiol.med.kyushu-u.ac.jp
Received 30 August 2010; revised 13 October 2010; accepted 27 October 2010.

METHODS

This study was reviewed and approved by the Committee of Ethics of Animal Experiments, Kyushu University Graduate School of Medical Sciences, and was conducted according to the Guidelines for Animal Experiments of Kyushu University.

Animals and General Procedures

Male Wistar-Kyoto/Izm rats (WKY) and spontaneously hypertensive/Izm rats (SHRs) (12–16 weeks old, SLC Japan, Hamamatsu, Japan) were used. Food and tap water were available *ad libitum* throughout the study. The rats were kept in a temperature- and humidity-controlled room under a 12-h light period between 8:00 AM and 8:00 PM. To obtain RVLM tissues, the rats were deeply anesthetized with sodium pentobarbital (100 mg/kg i.p.) and transcardially perfused with phosphate-buffered saline (150 mol/L NaCl, 3 mmol/L KCl, and 5 nmol/L phosphate; pH 7.4, 4°C). The brains were quickly removed, and 1-mm thick sections were obtained with a cryostat at −7±1°C. The RVLM was defined according to a rat brain atlas and the RVLM tissue was obtained using a punch-out technique, as previously described (6).

Microinjection into the RVLM

Spontaneously hypertensive rats and WKYs were initially anesthetized with sodium pentobarbital (50 mg/kg i.p., followed by a maintenance dosage of 20 mg/kg/h i.v.). A catheter was inserted into the femoral artery to record arterial blood pressure (AP) and heart rate (HR). A tracheal cannula was connected to a ventilator, and the rats were artificially ventilated. Body temperature was monitored with a rectal thermometer and maintained in the range of 36.5 to 37.5°C with a heating pad. The left kidney was exposed using a retroperitoneal approach, and the renal nerve prepared for recording renal sympathetic nerve activity (RSNA) as previously described (20). The rats were placed in a stereotaxic frame with the incisor bar and the dorsal surface of the medulla was surgically exposed to allow for positioning of the microinjection pipettes into the RVLM (with the pipette angled rostrally 18°, 1.8 mm lateral, 3.5 mm below the calamus scriptorius), as previously described (21). Microinjections (all microinjections were in a volume of 100 nL unless otherwise indicated) into the RVLM were made according to the following protocols: (1) unilateral microinjection of Ang-(1-7) (100 pmol); (2) bilateral microinjections of A-779 (100 pmol each); (3) unilateral microinjection of Ang-(1-7) (100 pmol each) 30 min after bilateral injections of A-779 (100 pmol each); (4) unilateral microinjection of Ang-(1-7) (100 pmol) 15 min after bilateral injections of AT_1 receptor antagonist valsartan (100 pmol each); (5) bilateral microinjection of ACE2 inhibitor DX600 (25 pmol in 50 nL each). Ang-(1-7) and A-779 were obtained from Bachem Inc. (Bubendorf, Switzerland). DX600 was obtained from Phoenix Pharmaceuticals (Burlingame, CA). The AT_1 receptor antagonist valsartan was a gift from Novartis Pharma AG (Basel, Switzerland). Drug doses were based on previous reports (9,15,19) or on preliminary experiments. Before microinjection of the drugs, the RVLM was identified by monitoring the mean arterial pressure (MAP) after injecting a small dose of L-glutamate. For bilateral injections, injections were first made on one side, and then the pipette was moved to the contralateral side; the two injections were made ~3 min apart. To verify the injection site histologically, 50 nL of Evans Blue dye was injected into the site at the end of the microinjection experiments. The rats were deeply anesthetized with an excessive dose of sodium pentobarbital, and transcardially perfused with 4% paraformaldehyde in phosphate-buffered saline. The brain was removed and sectioned to verify the microinjection sites. The rats whose microinjection sites were within the boundaries of the RVLM were used for data analysis.

Western Blot Analysis of the Mas Receptor in the RVLM

The RVLM tissue was homogenized and then sonicated in lysing buffer containing 40 mmol/L 4-(2-hydroxyethyl)-1-piperazineethanesulfonic acid (HEP ES), 1% Triton X-100, 10% glycerol, 1 mmol/L phenylmethanesulfonyl fluoride, and 1 mmol/L protease inhibitor cocktail tablet (Roche Diagnostics, Indianapolis, IN). The tissue lysate was centrifuged at 6000 rpm for 5 min at 4°C in a microcentrifuge. The lysate was collected and the protein concentration was determined using a bincinchoninic acid protein assay kit (Pierce, Rockford, IL). Aliquots of protein (50 μg) from each sample were separated on a 7.5% sodium dodecyl sulfate-polyacrylamide gel. Subsequently, the separated proteins were transferred onto polyvinylidene difluoride membranes (Immobilon-P membrane; Millipore, Billerica, MA). The membranes were incubated with goat IgG polyclonal antibody against Mas (1:1000; Santa Cruz Biotechnology, Santa Cruz, CA) and with rabbit IgG polyclonal antibody against GAPDH (1:1000; Santa Cruz Biotechnology) for 24 to 48 h. The membranes were then washed and incubated with horseradish peroxidase-conjugated horse anti-goat IgG or anti-rabbit antibody (1:10000; Santa Cruz Biotechnology) for 40 min. Immunoreactivity was detected by autoradiography using enhanced chemiluminescence and a western blotting detection kit (Amersham, Piscataway, NJ).

Statistical Analysis

All values are expressed as means ± SEM. The changes in MAP, HR, and RSNA values during the microinjection study were compared using a unpaired *t*-test or analysis of variance where appropriate. A P value of less than 0.05 was considered statistically significant.

RESULTS

Microinjection of Ang-(1-7) or A-779 into the RVLM

Unilateral microinjection of Ang-(1-7) into the RVLM increased AP in both strains, but the increase was significantly greater in SHR than in WKY ($P < 0.05$; Figures 1A and 1B). No significant changes in HR were observed in either strain. In contrast, bilateral microinjection of A-779 into the RVLM induced a significant decrease in AP and RSNA in both strains. The decreases in AP and RSNA were significantly greater in SHR than in WKY ($P < 0.05$; Figures 2A and 2B).

Effect of Valsartan or A-779 on the Ang-(1-7)-Induced Responses

Pretreatment with bilateral microinjection of A-779 into the RVLM attenuated the Ang-(1-7)-induced increase in AP (Figure 3A). Valsartan pretreatment did not change the Ang-(1-7)-induced increase in AP (Figure 3B).

Mas Receptor Expression in the RVLM

Mas receptor expression levels in the RVLM were significantly higher in SHR than in WKY ($P < 0.05$; Figure 4).

Microinjection of ACE2 Inhibitor DX600 into the RVLM

Bilateral microinjection of the ACE2 inhibitor, DX600, in the RVLM induced a significant decrease in AP in both strains. The decrease in AP was significantly greater in SHR than in WKY ($P < 0.05$; Figure 5).

DISCUSSION

The major findings of the present study were as follows: 1) the blockade of endogenous Ang-(1-7) in the RVLM

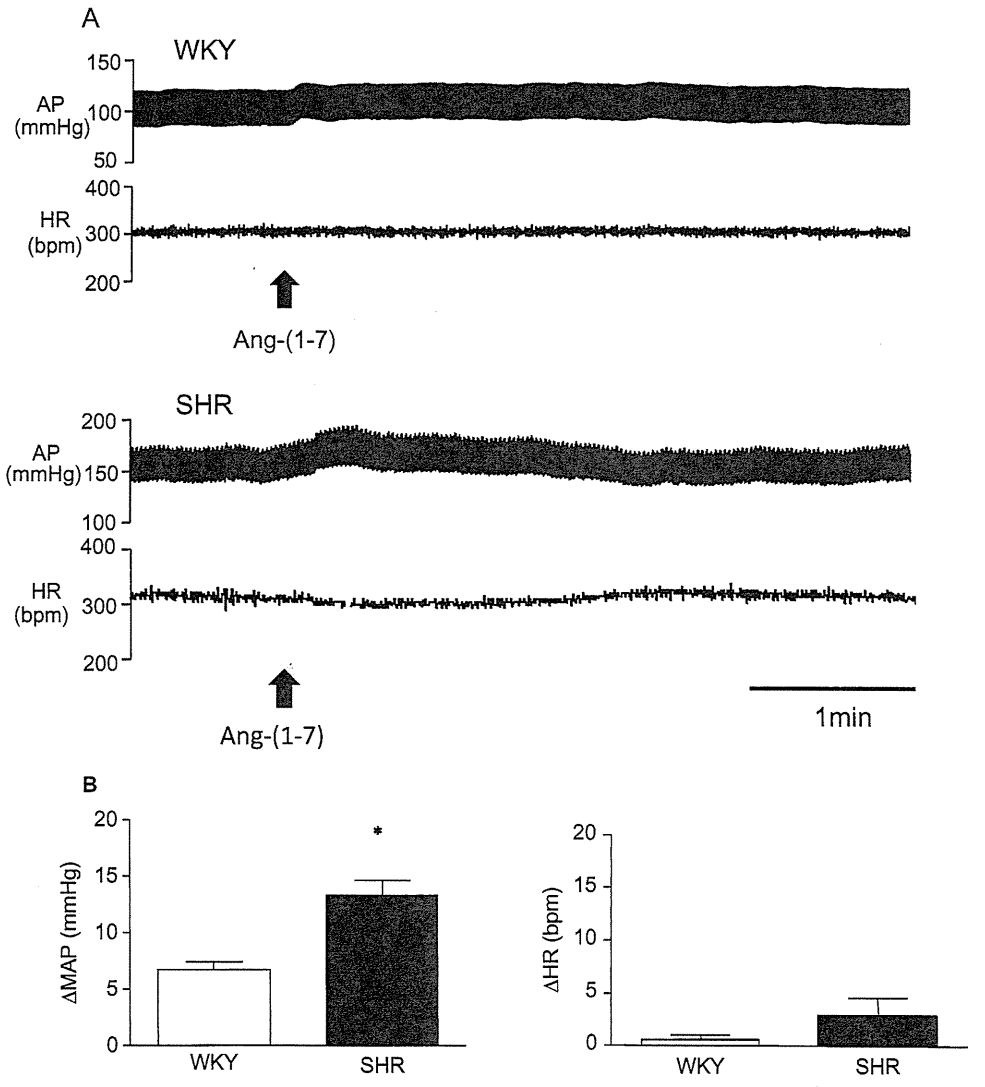

Figure 1. Effect of microinjection of Ang-(1-7) on arterial blood pressure (AP) and heart rate (HR). **A,** Changes in AP and HR after unilateral injection of Ang-(1-7) (100 pmol) into the rostral ventrolateral medulla (RVLM) in Wistar-Kyoto rats (WKY) (top) and spontaneously hypertensive rats (SHR) (bottom) rats. Arrow indicates the time at which Ang-(1-7) was injected. **B,** Grouped data of mean (+ SEM) change from baseline of AP (MAP) and HR evoked by unilateral microinjection of Ang-(1-7) into the RVLM. n = 6 per group. *$P < 0.05$ compared to WKY rats.